การสังเคราะห์ซิลิกาทรงกลมโดยวิธีโซลเจลและการประยุกต์ใช้เป็นตัวรองรับในตัวเร่งปฏิกิริยา

นายอนิรุตติ์ เล็กสมบูรณ์

วิทยานิพนธ์นี้เป็นส่วนหนึ่งของการศึกษาตามหลักสูตรปริญญาวิศวกรรมศาสตรมหาบัณฑิต
สาขาวิชาวิศวกรรมเคมี ภาควิชาวิศวกรรมเคมี
คณะวิศวกรรมศาสตร์ จุฬาลงกรณ์มหาวิทยาลัย
ปีการศึกษา 2553

SYNTHESIS OF SPHERICAL SILICA BY SOL-GEL METHOD AND ITS APPLICATION AS CATALYST SUPPORT

Mr.Anirut Leksomboon

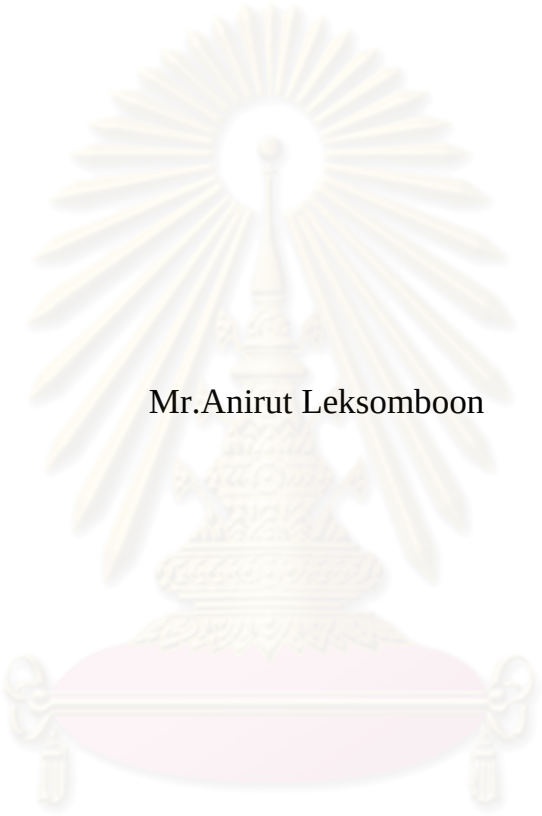

A Thesis Submitted in Partial Fulfillment of the Requirements
for the Degree of Master of Engineering Program in Chemical Engineering
Department of Chemical Engineering
Faculty of Engineering
Chulalongkorn University
Academic Year 2010

Thesis Title	SYNTHESIS OF SPHERICAL SILICA BY SOL-GEL METHOD AND ITS APPLICATION AS CATALYST SUPPORT
By	Mr. Anirut Leksomboon
Field of Study	Chemical Engineering
Thesis Advisor	Associate Professor Bunjerd Jongsomjit, Ph.D.

Accepted by the Faculty of Engineering, Chulalongkorn University in Partial Fulfillment of the Requirements for the Master's Degree

.....Dean of the Faculty of Engineering
(Associate Professor Boonsom Lerdhirunwong, Dr.Ing.)

THESIS COMMITTEE

.....Chairman
(Assistant Professor Anongnat Somwangthanaroj, Ph.D.)

.....Thesis Advisor
(Associate Professor Bunjerd Jongsomjit, Ph.D.)

.....Examiner
(Assistant Professor Joongjai Panpranot, Ph.D.)

.....External Examiner
(Assistant Professor Okorn Mekasuwandamrong, Ph.D.)

อนิรุตติ์ เล็กสมบูรณ์ : การสังเคราะห์ซิลิกาทรงกลมโดยวิธีโซลเจลและการประยุกต์ใช้เป็นตัวรองรับในตัวเร่งปฏิกิริยา. (SYNTHESIS OF SPHERICAL SILICA BY SOL-GEL METHOD AND ITS APPLICATION AS CATALYST SUPPORT) อ. ที่ปรึกษาวิทยานิพนธ์หลัก : รศ. ดร. บรรเจิด จงสมจิตร, 80 หน้า.

งานวิจัยนี้เสนอการศึกษาการสังเคราะห์ซิลิกาทรงกลมด้วยเตรตระเอทิลออกซิลไซแลน น้ำ สารละลายโซเดียมไฮดรอกไซด์ เอทิลลีนไกลคอล และโดเดคซิลไตรเมททิลแอมโมเนียมโบรไมด์ การควบคุมขนาดของอนุภาคทำได้โดยการปรับอัตราส่วนต่อน้ำหนักของตัวทำละลายร่วมเอทิลลีนไกลคอลของกระบวนการโซลเจล ในช่วงอัตราส่วน 0.10 ถึง 0.50 พบว่าอนุภาคที่ได้มีขนาดเพิ่มขึ้นเมื่อเพิ่มอัตราส่วนต่อน้ำหนักของตัวทำละลายร่วมเอทิลลีนไกลคอลแต่ค่าความสม่ำเสมอของขนาดอนุภาคลดลงและค่าความเบี่ยงเบนของขนาดอนุภาคมีค่ามากเมื่ออัตราส่วนต่อน้ำหนักของตัวทำละลายร่วมมากกว่า 0.35 และน้อยกว่า 0.15 อย่างไรก็ตามอนุภาคมีพื้นที่ผิวจำเพาะใกล้เคียงกันในทุกอัตราส่วนต่อน้ำหนักของตัวทำละลายร่วม มีค่าในช่วง 1000 ถึง 1300 ตารางเมตรต่อกรัม ซิลิกาทรงกลมที่สังเคราะห์มีพื้นที่ผิวจำเพาะสูง ตัวเร่งปฏิกิริยาโคบอลท์ถูกเตรียมบนซิลิกาทรงกลมเพื่อทดสอบปฏิกิริยาไฮโดรจิเนชันของคาร์บอนไดออกไซด์ พื้นที่ผิวจำเพาะของตัวเร่งปฏิกิริยาลดลงอยู่ในช่วง 400 ถึง 560 ตารางเมตรต่อกรัม โครงสร้างที่สม่ำเสมอและการกระจายตัวที่ดีทำให้ประสิทธิภาพของตัวเร่งปฏิกิริยาดีขึ้นทั้งต่อสารตั้งต้นและผลิตภัณฑ์ การปรับปริมาณโคบอลท์บนซิลิกาทรงกลมส่งผลต่อค่าความสามารถและค่าการเลือกเกิดของตัวเร่งปฏิกิริยา ที่อัตราส่วนปริมาณโคบอลท์เท่ากันพบว่าโครงสร้างที่สม่ำเสมอและขนาดของอนุภาคมีผลต่อประสิทธิภาพของตัวเร่งปฏิกิริยา นอกจากนี้การควบคุมลักษณะทางกายภาพและสัณฐานวิทยาของตัวรองรับมีผลต่อประสิทธิภาพการทำงานของตัวเร่งปฏิกิริยาโคบอลท์ในปฏิกิริยาไฮโดรจิเนชันของคาร์บอนไดออกไซด์

ภาควิชา...วิศวกรรมเคมี...ลายมือชื่อนิสิต...อนิรุตติ์ เล็กสมบูรณ์...

สาขาวิชา...วิศวกรรมเคมี... ลายมือชื่อ อ.ที่ปรึกษาวิทยานิพนธ์หลัก...ปรท...

ปีการศึกษา...2553...

5171480721: MAJOR CHEMICAL ENGINEERING
KEYWORDS : SPHERICAL SILICA, SOL-GEL METHOD, CARBON DIOXIDE HYDROGENATION

ANIRUT LEKSOMBOON: SYNTHESIS OF SPHERICAL SILICA BY SOL-GEL METHOD AND ITS APPLICATION AS CATALYST SUPPORT. ADVISOR: ASSOC. PROF. BUNJERD JONGSOMJIT, Ph.D., 80 pp.

In this present study, the spherical silica support was synthesized from tetraethyloxysilane (TEOS), water, sodium hydroxide, ethylene glycol and n-dodecyltrimethyl ammonium bromide (C_{12}TMABr). The particle size was controlled by variation of the ethylene glycol co-solvent weight ratio of a sol-gel method preparation in the range of 0.10 to 0.50. In addition, the particle size apparently increased with high weight ratio of co-solvent, but the particle size distribution was broader. The standard deviation of particle diameter was large when the co-solvent weight ratio was more than 0.35 and less than 0.15. However, the specific surface area was similar for all weight ratios ranging from 1000 to 1300 m^2/g. The synthesized silica was spherical and has high specific surface area. The cobalt was impregnated onto the obtained silica to produce the cobalt catalyst used for CO_2 hydrogenation. The specific surface area was reduced about 50 percentage in rang of 400 to 560 m^2/g. Uniformity and good dispersion provided higher efficiency of reactant and product exhibited in the result. The variation of catalyst loading significantly enhanced activity and selectivity of catalyst. The same catalyst loading was found to have a profound influence by uniformity of particle especially for the catalyst efficiency. Moreover, the control of the physical and morphology of support had effect on the performance of Co catalysts in CO_2 hydrogenation.

Department : Chemical Engineering	Student's Signature Anirut L.
Field of Study : Chemical Engineering	Advisor's Signature Bunjerd Jongsomjit
Academic Year : 2010	

ACKNOWLEDGEMENTS

The author would like to express his greatest gratitude and appreciation to his advisor, Associate Professor Bunjerd Jongsomjit for his invaluable guidance, providing value suggestions and his kind supervision throughout this study. In addition, he is also grateful to Assistant Professor Anongnat Somwangthanaroj, as the chairman, Assistant Professor Joongjai Panpranot and Assistant Professor Okorn Mekasuwandamrong as the members of the thesis committee. The author would like to thank the Thailand Research Fund (TFR).

Many thanks for kind suggestions and useful help to Mr. Jakrapan Janlamool, Mr. Benjapol Nitijalornwong, Miss Patsamol Rerksirikul and many friends in the laboratory who always provide the encouragement and co-operate along the thesis study.

Special thanks for all scientists in Center of Excellence on Catalysis and Catalytic Reaction Engineering, Faculty of Engineering, Chulalongkron University for support the equipment technique in characterization tests.

Most of all, the author would like to express his highest gratitude to his parents who always pay attention to his all the times for suggestions, support and encouragement.

CONTENTS

CHAPTER Page

Page

LIST OF TABLES

LIST OF FIGURES

CHAPTER I

INTRODUCTION

Silica (SiO_2) is one of the main catalyst supports that has been used widely on heterogeneous catalysts. It had more surface area and has been widely used in various manufacturing industries, such as used to the supports of vanadium oxide (V_2O_5) and other oxides catalyst in the sulfur dioxide oxidation reaction [Giakoumelou et al., 2004], supported of chromium oxide catalyst in the reaction produced of poly ethylene (Philip Catalyst), support of copper / zinc oxide catalyst in the reaction of CO_2 hydrogenation [Kusama et al., 1996], support of cobalt / titania oxide catalyst in the Fischer-Tropsch reaction [Hinchiranan et al., 2008] etc. The main topic of research into silica (SiO_2) materials is uniformity of the shape, pore volume and the specific surface area. Among particles with all kinds of morphology, monodispersed silica spheres are very promising because of many applications in the area of catalysis and absorbents. The porous silica was synthesized and classified as mesoporous silica or submi-croporous silica according to the diameter of the pore.

The method of synthesis silica has been produced silica in typically several products such as fibers, films, polyhedral particle, spheres [Yang, 1998; Tolbert, 1997; Shunai, 2001; Kosuge, 2001] etc. Meanwhile, the good structure of silica may lead to great accessibility to utilize the active site for catalyst reaction. Silica sphere has been synthesized by various methods, such as using cationic surfactant under acidic condition, using nonionic surfactant as a template under static and acidic condition, by addition of CTBA as co-surfactant or using the two step synthesis by pH adjustment and addition of small amount of fluoride as catalyst. [Yang et al., 2006]

It has become possible to synthesize silica by the sol-gel method. The synthesis of monodispersed mesoporous silica spheres by modifying the Stöber procedure. The particle was reacting with emulsion / phase separation system by additional silica source, water, alcohol, and the further addition of the surfactant template such as and alkyl amine. The synthesis has been extended control the diameter and pore size of particle. However, the method for preparation mesoporous silica spheres with uniform particle size and good dispersibility are still required.

The combustion of fossil fuel, deforestation and human activity have increased the atmospheric concentration of carbon dioxide about 35 % since the age of industrialization was began. Carbon oxide and carbon dioxide exhibit the noticeable problem in the life, such as the lost of oxygen carrier molecule in red blood cell of human metabolism, activated the more acid rain and the main cause of global warming. Therefore, cobalt supported on silica has been subject of many studies. During the past 10 years cobalt based catalysts appear as the most popular system for Fischer-Tropsch and carbon oxide hydrogenation [Borodko and Somorjai, 1999]. The catalytic hydrogenation of the carbon oxide and carbon dioxide produced a large variety of products ranging from methane and methanol (C1 products) to higher molecular weight alkanes, alkenes and alcohols, a process that requires C–C bond formation as well [Somorjai , 1994; Dry, 1996; Adesina, 1996;Iglesia, 1997]. In recently, carbon monoxide is a very small amount trace gas being about 0.1 ppm in atmosphere. Then, carbon dioxide is the most abundant carbon source in the atmosphere for catalytic hydrogenation.

Many researches were investigated the metallic/bimetaric support and promoter effect to the activity and selectivity of hydrocarbon formation. The previous research showed that the synthesis reaction on metallic cobalt is an excellent catalyst for Fischer-Tropsch and carbon oxide hydrogenation [Okabe, 2004; Panagiotopoulou, 2008]. However, the effect of physical and chemical properties of support on the performance of Co catalysts in Fischer-Tropsch and carbon oxide synthesis still remains unclear [Li et al., 2006].

The present work describes the synthesis of silica spheres with silica source of tetraethyloxysilane (TEOS) and n-dodecyltrimethyl ammonium bromide (C_{12}TMABr) as a surfactant template in a sol-gel method in alkali aqueous solution. The morphology and size of particle were controlled with the ethylene glycol co-solvent weight ratio of variation in the range of 0.10 to 0.50. The silica spheres were used in catalyst support of Co/SiO_2 and prepared by the incipient wetness technique. The silica sphere support and catalyst were characterized by X-ray diffraction (XRD), scanning electron microscopes (SEM) and energy dispersive X-ray spectroscopy (EDX), transmission electron microscope(TEM), temperature-programmed reduction

(TPR), nitrogen physisorption (BET surface areas), differential thermal analysis and themogravimetric (DTA/TG), CO chemisorptions isotherm. The activity and selectivity of catalyst was tested for the CO_2 hydrogenation when amounts of hydrocarbon product are generated. It is proposed here a sol-gel method to introduce silica into spherical support. As an application of this kind of support diameter and physical properties are in direct contact in performance of the CO_2 hydrogenation.

Motivation

A silica spherical particle is one of favorite supports for heterogeneous catalysts in many reactions. On the other hand, silica spheres were used in adsorbent material, separate substances in separation column, materials substance in medical clinical and cosmetics. So the spherical silica as commercial material was expensive. The above studies indicated that the physical and chemical properties of catalyst affect product selectivity. Moreover, silica spheres were synthesized by the general method having the amorphous shape and more probability of uncertainty of surface area. In this work, the method was used to improve uniformity of the shape, pore volume and the specific surface area of silica spherical support. The efficiency result obtained the product (activity and selectivity) on the performance of Co catalysts based variation size of SiO_2 in CO_2 hydrogenation.

Objective

This research objective is to investigate the effect of different particle size of spherical silica supports on their physical and chemical properties as the catalyst support. The cobalt was impregnated onto the obtained spherical silica to produce the cobalt catalyst used for CO_2 hydrogenation.

Research Scopes

- Preparation of spherical silica by sol-gel method [Yamada and Yano., 2006] from tetraethyloxysilane (TEOS) as a silica source, water, sodium hydroxide, ethylene glycol and n-dodecyltrimethyl ammonium bromide (C_{12}TMABr) as a surfactant template. The particle size was controlled by variation of the ethylene glycol co-

solvent weight ratio of a sol-gel method preparation in the range of 0.10 to 0.50 (7 series products).

-Characterization of silica support samples by BET surface area, scanning electron microscopy (SEM), transmission electron spectroscopy (TEM) and X-ray diffraction (XRD)

- Preparation of Co/SiO_2 catalyst with 20 wt% of Co by the incipient wetness impregnation.

- Characterization of the Co/SiO_2 catalyst supports by BET surface area, X-ray diffraction (XRD), scanning electron microscopy (SEM), energy dispersive X-ray spectroscopy (EDX), transmission electron spectroscopy (TEM), temperature-programmed reduction (TPR), differential thermal analysis and thermogravimetric (DTA/TG) and CO chemisorptions isotherm.

- Investigation of the catalytic activity of each Co/SiO_2 catalyst in the hydrogenation of carbon dioxide (CO_2) at 220^oC and 1 atm and a H_2/CO_2 ratio of 10 under methanation condition.

- Supported Co catalysts on the SiO_2 supports were synthesized by variation of the ethylene glycol co-solvent weight ratio 0.10 with 5wt% and 10 wt% of Co by the incipient wetness impregnation.

- Supported Co catalysts on the SiO_2 supports were synthesized by variation of the ethylene glycol co-solvent weight ratio 0.50 with 5wt% and 10wt% of Co by the incipient wetness impregnation.

- Characterization of the Co/SiO_2 catalyst supports by BET surface area, X-ray diffraction (XRD) scanning electron microscopy (SEM), transmission electron spectroscopy (TEM), temperature-programmed reduction (TPR), differential thermal analysis and thermogravimetric (DTA/TG) and CO chemisorptions isotherm.

- Investigation of the catalytic activity of Co/SiO_2 catalyst in the hydrogenation of carbon dioxide (CO_2) at 220^oC and 1 atm and a H_2/CO_2 ratio of 10 under methanation condition.

Benefits

-Develop the morphology and uniformity of the shape of silica used as the catalyst support for heterogeneous catalysts.

- Decrease the expensive value of silica support commercial by easier preparation method as well as good the physical and chemical properties for supported heterogeneous catalysts.

CHAPTER II

LITERATURE REVIEWS

Over few century years after the discovery of mesoporous materials, great efforts have been made to modify a control of mesoporous structures. These materials have been approached on their versatile application in catalysis, separation, and drug delivery. Recently, one of the interesting subjects in mesoporous materials is the synthesis of mesophase structures with controllable morphologies for the purpose of industrial applications. Since the first study in sol–gel synthesis which the formation of mesoporous silica spheres was reported through a modification of Stöber's procedure many kinds of mesoporous silica spheres have been introduced. The preparation of spherical mesoporous particles in the micrometer-size range has received much attention because of packing easily into reactors, columns, or diverse systems [Kurganov et al., 1996].

This chapter reviews the work about silica sphere support method preparation that is also of great interest in the field of heterogeneous catalysts. Metal oxide catalyst base on SiO_2 has been used for some catalytic application and the last section of this review shows a few research investigations about the silica support/bisupport metal catalyst in carbon oxide hydrogenation.

2.1 The silica support preparation

The synthesis of mono-dispersed silica spheres was first conducted by Stöber in 1968. There was employing a water–alcohol–ammonia–tetraalkoxysilane system [Stöber and Fink, 1968]. The silica product was mesoporous particle and good dispersion. For 20 years ago, the researched about MCM-41 was published [Tsuneo et al., 1990] for produced the SiO_2 networks products of the complexes had micro pores 2-4 nm in diameter and morphology was amorphous. It has attracted much attention because of its emerging applications in the areas of catalysis, adsorption, chromatography, and controlled release of drugs. [Davis, 2002; Stein, 2003]

Grün et al. [1997] were made to synthesize mesoporous silica spheres by modifying the Stöber method with further addition hexadecyltrimethylammonium

bromide (C_{16}TMABr) or hexadecyltrimethylpyridinium chloride (C_{16}TMPrCl) as a surfactant with distorted shape. So far, few reports exist for the synthesis of mesoporous silica spheres that consist of both uniform spherical morphology and ordered mesoporous hexagonal regularity. Recently, ordered mesoporous silica having high specific surface area was synthesized by modifying the Stöber method using a template such as an alkyl amine [Luo et al., 2000]. However, although the spheres formed were very fine, the materials were poorly ordered with lower specific surface areas and pore volumes.

Previous scientist report that MCM-41 has been use tetra-n-alkoxysilanes such as tetraethoxysilane (TEOS) or tetra-n-propoxysilane (TPS) as a silica source which are added to an aqueous solution of a cationic surfactant in the presence of ammonia as catalyst to produced mesoporous silicate and aluminosilicate [Beck et al., 1992]. It was previously report that the particles product is high of specific surface area, specific pore volume and the mean pore diameter into 2-10 nm. Beside, the report shown that uniformity of particle was combine hexagonal regulatory and amorphous mixture. However, the more specific surface area and specific pore volume of product was incentive many research has been made to modified and improve their morphology.

Next, Grün et al. [1999] proposed the preparation of mesoporous MCM-41 materials. The methods use n-alkyltrimethylammonium bromides and n-alkylpyridinium chlorides were employed as templates. The addition of an alcohol (e.g. ethanol or isopropanol) leads to a homogeneous system which allows the formation of spherical MCM-41 particles. The main advantages of these methods are short reaction times, excellent reproducibility and easy preparation of large batches. Recently, Agren et al. [1998] found the adding effect of polyethylene glycol (PEG) as a co-absorbance of silica in acid solution to prepared spherical silica by colloidal silica particles (sol-gel method). It was found that polyethylene glycol (PEG) accelerated the formation and flocculation of colloidal silica particles under temperature condition.

Kosuge et al. [2001] describes the effect of adding 1-alkylamine under acidic conditions to synthesize the mesoporous silica spheres in size mean diameter about

100 μm. It shows that 1-alkylamine was wizard the structure-directing agent through the S+X−I+ assembly pathway. Future more, Yano and Fukushima [2003] were investigated the spherical silica by Stöber procedure with tetraalkoxysilane (TMOS) as silica source and n-alkyl trimethylammonium bromide (CnTMABr) were used in combination, and it was found that ordered mono-dispersed mesoporous silica spheres with a highly uniform particle size. The result exhibited the shorter the alkyl-chain length of the surfactant was, such as in the order of C_{16}, C_{14} and C_{12}, more good morphology with decrease the shorter alkyl-chain length became. Therefore, the results was showed the particle size of mono-dispersed super-microporous silica spheres synthesized from tetramethoxysilane (TEOS) and the short alkyl-chain length of n-decyltrimethylammonium bromide (C_{10}TMABr) was successfully controlled their mono-dispersion characteristics. The variation of the C_{10}TMABr / TEOS ratio in solvent affected to the morphology and dispersion of mesoporous silica. However, the C_{10}TMABr / TEOS ratio in solvent less than 0.63 showed the uniformity of mono-dispersed spherical particle and were not significantly effect to particle diameter. Beside, the average diameter of particle were affected by temperature, silica source and methanol/water ratio in solvent.

Next, Kosuge et al. [2004] reported that carried out a one-step selective preparation of monodispersed mesoporous and microporous dominant spheres with a diameter of 130–225 μm using a commercial sodium silicate solution and various Pluronic triblock copolymers. Schacht et al. [1996] demonstrated that mesoscopically ordered hollow spheres could be prepared by interfacial reactions conducted in oil/water emulsions with varying extents of imposed shear. Micrometer- and millimeter-sized hollow silica spheres have also been produced by the controlled hydrolysis of silicon alkoxides in stabilized emulsions of biphasic systems. However, the research does not show the silica particles have been increased uniform spherical morphology and satisfactory particle size distribution.

Futuremore, Yano and Fukushima [2006] was successfully synthesized of monodispersed super-microporous/mesoporous silica spheres with particle diameters falling in the range 0.1–0.4 μm from tetramethoxysilane (TMOS) and n-dodecyltrimethylammonium bromide. By using polyol, rather than methanol, as a co-

solvent, the particle diameters were reduced. Moreover, the addition of a polymer contributed to the decrease in particle diameter. It was assumed that the increased solution viscosity led to a higher generation of primary particles, resulting in smaller particle diameter. Furthermore, it was found that a colloidal crystal film fabricated from the monodispersed mesoporous silica spheres obtained using ethylene glycol as a co-solvent reflects light in the visible light region.

Yang et al. [2006] proposed the preparation of micrometer-sized silica spheres were using a new pH-induced rapid colloid aggregation method in water-in-oil (W/O) emulsion separately with F127 and the mixture of pluronic triblock copolymer (F127, P123, or P105) and PEG20000 as templates. It was exhibited high surface areas (657–1145 m^2/g) and large pore volumes (0.46–2.16 ml/g) of all the mesoporous silica spheres. But the synthetic condition has been uniform silica morphology out of monostructure/monodispersed pattern.

Zhang et al. [2008] investigated the polyethylene glycol (PEG) and methyl cellulose (MC) has been added to liquid crystal in aqueous solution. The morphology of micrometer-sized mesoporous silica spheres with good dispersivity were synthesized by adding the mixture of PEG and MC into the aqueous solution containing F127 and TEOS. It was found that only when PEG was added the spheres possess. The mesoporous silica was increased specific surface area and meso-pores diameter by changing the amount of PEG, but the mesoporous silica has been low dispersibility. Only when MC was added, the dispersibility of resultant spheres was good, but the out surface of spheres was not smooth. The adding suitable amount of PEG and MC were simultaneously obtained the spheres with good dispersibility and smooth out surface.

2.2 The support metal catalyst in carbon oxide hydrogenation system

The catalytic hydrogenation of carbon monoxide and carbon dioxide produces a large variety of products ranging from methane and methanol to higher molecular weight alkanes, alkenes and alcohols [Somorjai, 1994]. Development of catalyst for CO and CO_2 hydrogenation in the surface science studies is the key technology of gas to liquid (GTL) process. The presence of prepared a group of Ni/Al_2O_3 catalysts

having metal contents in the 0-16.5 wt% range using coprecipitation and impregnation methods. The CO and CO_2 methanation activities of the catalyst were studied in order to compare the effect of preparation method on structure properties as well as on catalyst activity and selectivity. The comparison of Co hydrogenation results in catalyst with similar nickel loading indicates that coprecitated catalysts have higher productivity and C2-C4 hydrocarbon selectivity, whereas impregnated catalysts yield better olefin/paraffin ratios for the C2-C4 hydrocarbons. In CO_2 methanation, coprecipitation shows higher methanation activity for all nickel loadings. [Aksoylu et al., 1997]

In resent year, Chang et al. [2003] illustrated nickel catalysts supported on rice husk ash-alumina (Ni/RHA-Al_2O_3) using the incipient wetness impregnation method. The nickel catalysts has been tested the catalytic activities by CO_2 hydrogenation in 4:1 ratio of H_2/CO_2 for temperatures between 400 and 800^oC. The TPR analysis indicated that the interaction between nickel and support was strong and difficult to reduce with more than one nickel oxide compound. The CO_2 conversion and CH_4 yield for CO_2 hydrogenation were found to depend on the nickel loading. The reaction temperature of 500^oC might be the optimum temperature for CO_2 hydrogenation to give the maximum yield and selectivity of CH_4.

Furthermore, Okabe et al. [2004] investigated the Fischer-Tropsch synthesis that was carried out in slurry phase over uniformly dispersed Co/SiO_2 catalysts prepared by sol-gel method. When 0.01-1 wt% of noble metals were added to the Co/SiO_2 catalysts, a high and stable catalytic activity was obtained over 60 h of the reaction at 230°C and 1 MPa. The addition of noble metals increased the reducibility of surface Co on the catalysts, without changing the particle size of Co metal. The uniform pore size of the catalysts was enlarged by varying the preparation conditions. Increased pore size resulted in decreased CO conversion and selectivity for CO_2 and increased olefin/paraffin ratio of the products. Takanabe et al. [2005] prepared titania supported cobalt and nickel bimetallic catalysts for CO_2 reforming of methane to synthesis gas at 750°C under ambient pressure. Bimetallic Co-Ni/TiO_2 catalysts with an appropriate Co/Ni ratio show highly stable activities without carbon deposition. Whereas the monometallic Co/TiO_2 catalyst deactivated rapidly because of the

oxidation of metal, 10% mol substitution of nickel for cobalt suppressed the oxidation of metal, providing a high catalytic stability. The advantages of the bimetallic catalysts are high resistance to undesirable metal oxidation and coaking through the control of reactions between CH_4 and CO_2.

Jongsomjit et al. [2006] illustrated the affect of mixed TiO_2-SiO_2 with various weight ratio of TiO_2/SiO_2, supported cobalt in Fischer–Tropsch synthesis. The initial and steady state rates decreased with the amounts of titania present in mixed supports that had the less number of reduced cobalt metal. The selectivity of long chain hydrocarbons (C2-C5) was increased with the presence of titania in the mixed supports. Furthermore, Jongsomjit et al. [2005] investigated influence of various titania/silica mixed-oxides supported MAO on the catalytic activity copolymerization of ethylene and 1-hexane with zirconocene catalyst. The activity, that had titania range between 20 and 40% in the mixed oxide supports, increased up to 30% compared with pure silica.

Panagiotopoulou et al. [2008] investigated that the catalytic performance of Al_2O_3 supported noble metal catalysts for the methanation of CO, CO_2 and their mixture with respect to the nature of the dispersed metallic phase (Ru, Rh, Pt, Pd). It has been found that, for all experimental conditions investigated, Ru and Rh are significantly more active than Pt and Pd. Selectivity towards hydrogenation products depends strongly on the noble metal catalyst employed as well as on whether solo- or co-methanation of Co/ CO_2 is occurring. In present of water in the feed, catalytic activity of Ru is not affected, while that of Rh is reduced. On the other hand, the performance of Pt and Pd is poor since they promote the undesired water-gas shift reaction.

CHAPTER III

THEORY

3.1 Sol-gel method

The sol-gel process is involves the evolution of inorganic networks through the formation of a colloidal suspension (sol) and gelation of the sol to form a network in a continuous liquid phase (gel). The precursors for synthesizing these colloids consist usually of a metal or metalloid element surrounded by various reactive ligands. The starting material is processed to form a dispersible oxide and forms a sol in contact with water. Removal of the liquid from the sol yields the gel, and the sol/gel transition controls the particle size and shape.

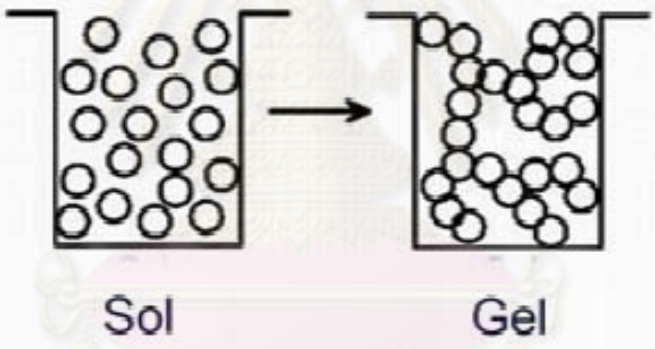

Figure 3.1: The evolution of sol-gel

The interest in sol-gel processing can be traced back in the mid-1980s with the observation that the hydrolysis of tetraethyl orthosilicate (TEOS) under acidic conditions led to the formation of SiO_2 in the form of fibers and monoliths. Sol-gel research grew to be so important that in the 1990s [Hench et al., 1990]. The synthesis method arises due to the possibility of synthesizing nonmetallic inorganic materials at very low temperatures. The initial system represents a solution where different polymerization and polycondensation process lead to the gradual formation of the solid phase network.

Sol-gel processing refers to the step of hydrolysis and condensation of alkoxide-based precursors such as tetraethyl orthosilicate (TEOS). The reactions involved in the sol-gel chemistry based on the hydrolysis and condensation of water and alcohol has been described as follows:

Hydrolysis : M-O-R + H_2O ⟶ M-OH + R-OH

Water Condensation : M-OH + HO-M ⟶ M-O-M + H_2O

Alcohol Condensation: M-O-R + HO-M ⟶ M-O-M + R-OH

When M = Metal such as Si, Zr, Ti, Al, Sn, Ce

R = Alkoxyl Group (C_2H_5)

First, the process was formation of different stable solutions of the alkoxide or solvated metal precursor.

Figure 3.2: Hydrolysis reaction of sol-gel

The gelation resulting from the formation of an oxide- or alcohol- bridged network that results in a dramatic increase in the viscosity of the solution.

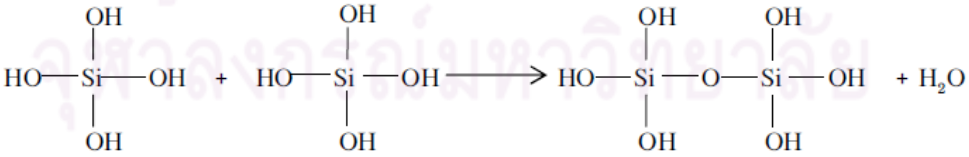

Figure 3.3: Water condensation reaction of sol-gel

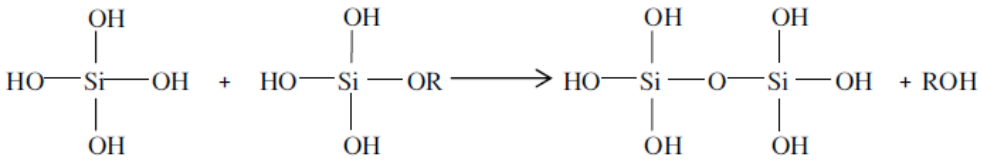

Figure 3.4: Alcohol condensation reaction of sol-gel

Next, during which the polycondensation reactions continue until the gel transforms into a solid mass, accompanied by contraction of the gel network and expulsion of solvent from gel pores.

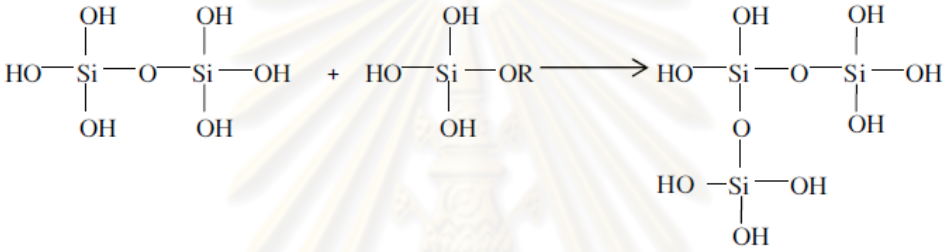

Figure 3.5: Polycondensation/Polymerization reaction of sol-gel

Finally, drying, dehydration or densification of the gel, when water and other volatile liquids are removed from the gel network. This process is complicated due to fundamental changes in the structure of the gel.

3.2 Silicon dioxide (SiO_2)

Silicon dioxide or silica is an oxide of silicon with the chemical formula SiO_2. It has been used in many fields since antiquity. Silica is most commonly found as sand or quartz in the nature.

Table 3.1: Physical properties of silica

Parameter	Properties
Other names	Silica
Molecular formula	SiO_2
Molar mass	60.1 g/mol
Appearance	white or colorless solid (when pure)
Status	solid at atmosphere
Density and phase	2.6 g/cm^3
Melting point	1610 °C
Boiling point	2230 °C
Solubility	insoluble in water
	insoluble in acid chloride

Silica has been used in the many varied forms before the ancient time. Because of its many form, silica has been called by more names than any other mineral. Some of the older names of flint are now so obsolete that repetition is needless, but many of the present-day names for quartz gems are unknown save to a few jewelers. Then, too, the exact research of the modern laboratory has shown several distinct crystallographic varieties of silica; some of which are closely connected with the temperatures experienced in their life-history.

The many different names are now in use for silica minerals, call for a classification and arrangement in a more ample, yet more concise manner than is to be found in the usual discussion of the varieties of silica. This article is written with the hope of making a scientific classification of these names, so that the use of the different terms will no longer be a cause for tedious searching for definitions.

The classification of silica was changes the recrystallization formed with descending temperatures. Besides the changes at these critical temperatures, there are probably similar changes from unstable forms towards quartz at atmospheric temperatures, especially after long time intervals. With fairly rapid cooling or heating intermediate forms may not occur in their stable zone, but a direct change from one to another without the intermediate product may take place. Most of the recrystallization changes noted are found to occur at the ascending and descending temperatures.

(A) SILICA GLASS - amorphous, a true non-crystalline glass, stable below the melting point and above the "gc" temperature. Quartz Glass, Fused Silica, Fused Quartz, are other names for this supercooled liquid. In most forms at atmospheric temperatures there are traces of cristobalite.

(B) CRISTOBALITE - isometric, or pseudo-isometric, "gc" range is at 1710° where Cristobalite changes to glass as temperatures rise, or glass to cristobalite as they fall. Christobalite, an alternate spelling. Beta Cristobalite, also called High Cristobalite, is the high temperature product, forming in the "gc" range in cooling. It is isometric, and in cooling recrystallizes to Alpha Cristobalite, or Low Cristobalite, at 200-275°, providing cooling through the "ct" and "tq" ranges has been too rapid for recrystallization. It is tetragonal.

(C) TRIDYMITE - hexagonal, bipyramidal. "ct" range is at 1470°, where cristobalite changes to tridymite on cooling. Glass may crystallize as tridymite at 1670° if the cooling was too rapid through the "gc" range. Beta Second Tridymite, or Upper High Tridymite, is the high temperature product, forming in the "ct" range in cooling, and which recrystallizes to Beta First Tridymite, also called Lower High Tridymite, at 163° if cooling was too rapid for the "tq" transformation. This in turn alters to Alpha Tridymite, or Low Tridymite, at 117°, which is the usual tridymite of nature.

Asmanite	- a meteoric tridymite, related to the above series.
Vestan	- a doubtful silica mineral, probably to be ascribed to tridymite.

Granuline - a doubtful pulverescent mineral which seems allied to tridymite on optical grounds.

(D) QUARTZ - hexagonal, forms from tridymite in the "tq" range at 870° in cooling. Glass may change to crystalline quartz at about 1400° providing cooling was too rapid for the "gc", "gt" and "ct" transformations. Beta Quartz, or High Quartz, is the high temperature product, forming at the "tq" point. It is hemihedral. On cooling it recrystallizes to Alpha Quartz, also called Low Quartz, at 573°, yielding the stable low temperature mineral. It is tetartohedral, showing polarity along the c axis and is divisable into Right Hand Quartz and Left Hand Quartz.

(E) CHALCEDONY - a cryptocrystalline, or very finely fibrous mineral, which has not been successfully located in the thermal equilibrium diagram. Heating to 725-850° usually results in an alteration to tridymite, which thereafter acts as normal tridymite. Chalcedony is usually found as a deposit from solutions, and may be a mixture of glass and quartz, or more probably an intermediate product in the dehydration of the opal colloid. Various subdivisions of chalcedony have been made on optical grounds.

Chalcedony - biaxial, positive, elongationpositive.

Chalcedonite - biaxial, negative.

Lussatite - biaxial, positive, parallel, elongation.

Quartzine - biaxial, positive, negative elongation, pseudochalcedonite, Lutecite.

Jenzschite - differently soluble, but of same S. G. as chalcedony.

Melanophlogite - possibly impure chalcedony.

Sulfuricin - probably a chalcedony rich in sulphur.

(F) COLLOIDAL SILICA - is usually hydrous, and is commonly described under opal. Silicon occurs in nature combined with oxygen in various forms of silica and silicates. Silicates have complex structures consisting of SiO_4 tetrahedral structural units incorporated to a number of metals. Silicon is never found in nature in free elemental form. Among all elements silicon forms the third largest number of

compounds after hydrogen and carbon. There are well over 1000 natural silicates including clay, mica, feldspar, granite, asbestos, and hornblende. Such natural silicates have structural units containing orthosilicates, SiO_4^{4-}, pyrosilicates $Si_2O_7^{6-}$, and other complex structural units, such as, $(SiO_3)_n^{2n-}$ that have hexagonal rings arranged in chains or pyroxene $(SiO_3)_n$ and amphiboles, $(Si_4O_{11}^{6-})_n$ in infinite chains. Such natural silicates include common minerals such as tremolite, $Ca_2Mg_5(OH)_2Si_8O_{22}$; diopside, $CaMg(SiO_3)_2$; kaolin, $H_8Al_4Si_4O_{18}$; montmorillonite, $H_2Al_2Si_4O_{12}$; tale, $Mg_3[(OH)_2SiO_{10}]$; muscovite (a colorless form of mica), $H_2KA_{l3}(SiO_4)_3$; hemimorphite, $Zn_4(OH)_2Si_2O_7.H_2O$; beryl, $Be_3Al_2Si_6O_{18}$; zircon, $ZrSiO_4$; benitoite, $BaTiSi_3O_9$; feldspars, $KAlSi_3O_8$; zeolites, $Na_2O.2Al_2O_3.5SiO_2.5H_2O$; nephrite, $Ca(Mg,Fe)_3(SiO_3)_4$; enstatite, $(MgSiO_3)n$; serpentine, $H_4Mg_3Si_2O$, jadeite, $NaAl(SiO_3)_2$; topaz, $Al_2SiO_4F_2$; and tourmaline, $(H,Li,K,Na).Al_3(BOH)_2SiO_{19}$. silica, theother most important class of silicon compounds, exists as sand, quartz, flint, amethyst, agate, opal, jasper, and rock crystal.

3.3 Cobalt

Cobalt is a transition metal element with symbol Co and atomic number 27. Cobalt is similar to silver in appearance. Cobalt and cobalt compounds have been used since ancient times for jewelry and paints pigments. Cobalt have expended from use colorants inglasses and ground coat frits for pottery to drying agents in paints and lacquers, animal and human nutrients, electroplating materials, high temperature alloys, hard facing alloys, high speed tools, magnetic alloys, alloys used for prosthetics, and used in radiology. In recent year, some cobalt is produced specifically from various metallic-lustered ores. In the other there, Cobalt is also as a catalyst for reaction of hydrocarbon refining from crude oil for the synthesis of heating fuel.

Table 3.2: Physical properties of cobalt

Parameter	Property
Name	cobalt
Symbol	Co
Electron configuration	[Ar]3$d^7$4s^2
Atomic number	27
Atomic weight 5	8.93
Melting point, ^oC	1493
Boiling point, , ^oC	3100
Transformation temperature, ^oC	417
Heat of transformation, J/ga	251
Latent heat of fusion, ΔHfus J/ga	395
Latent heat of vaporization at bp, ΔHvap kJ/ga	6276
Specific heat, J/(g.^oC)[a]	
15-100^oC	0.442
Molten metal	0.560
Coefficient of thermalexpansion, ^oC	-1

Table 3.2: (cont.) Physical properties of cobalt

Parameter	Property
cph at room temperature	2.5
fcc at 417^{o}C	14.2
Thermal conductivity at 25^{o}C, W/(m.K)	69.16
Thermal neutron absorption, Bohr atom	34.8
Resistivity, at 20^{o}C[b], 10^{-8} Ω.m	6.24
Curie temperature, ^{o}C	1121
Saturation induction, 4πIs, T[c]	1.870
Permeability, μ	
initial	68
max	245
Residual induction, T[e]	0.490
Coercive force, A/m	708
Young's modulus, Gpac	211

The scale formed on unalloyed cobalt during exposure to air or oxygen at high temperature is double-layered. In the range of 300 to 900^{o}C, the scale consists of a thin layer of mixed cobalt oxide, Co_3O_4, on the outside and cobalt (II) oxide, CoO, layer next to metal. Cobalt (III) oxide, Co_2O_3, may be formed at temperatures below 300^{o}C. Above 900^{o}C, Co_3O_4 decomposes and both layers, although of different appearance, are composed of CoO only. Scales formed below 600^{o}C and above 750^{o}C appear to be stable to cracking on cooling, whereas those produced at 600-750^{o}C crack and flake off the surface.

Cobalt forms numerous compounds and complexes of industrial importance. Cobalt, atomic weight 58.933, is one of the three members of the first transition series of Group 9 (VIIIB). There are thirteen know isotopes, but only three are significant,

Co is the only stable and naturally occurring isotope, Co has a half-life of 5.3 years and is a common source of γ-radioactivity; and ^{57}Co has a 270-d half-life and provides the γ-source for Massbauer spectroscopy.

Cobalt exists in the +2 or +3 valance states for the major of its compounds and complexes. A multitude of complexes of the cobalt (III) ion exists, but few stable simple salt are known. Octahedral stereochemistries are the most common for cobalt (II) ion as well as for cobalt (III). Cobalt (II) forms numerous simple compounds and complexes, most of which are octahedral or tetrahedral in nature; cobalt (II) forms more tetrahedral complex than other transition-metal ions. Because of the small stability difference between octahedral and tetrahedral complexes of cobalt (II), both can be found equilibrium for a number of complexes. Typically, octahedral cobalt (II) salts and complexes are pink to brownish red; most of the tetrahedral Co (II) species are blue.

3.4 CO_2 Hydrogenation Reaction

In recently, several reaction mechanisms for the CO_2 hydrogenation have been proposed. First, the catalytic hydrogenation over promoted Cu-ZnO catalysts under pressurized conditions produces mainly CH_3OH, CO and H_2O. A small amount of CH_4 was produced. At higher temperature, a very small amount of CH_3OCH_3 was also produced. Therefore, main reactions are shown in the following equations [Arakawa et al., 1992].

$$CO_2 + 3H_2 \rightleftharpoons CH_3OH + H_2O$$

$$CO_2 + H_2 \rightleftharpoons CO + H_2O$$

An in situ FT-IR observation of surface species over 5 wt% Cu-ZnO/SiO_2 as model catalyst showed the presence of bidentate carbonate species on both Cu and ZnO at the condition of 3 MPa, 30^{o}C and 100 ml/min. Also a small amount of adsorbed CO on Cu site was observed. These bidentate carbonate species were rapidly transformed to the bidentate formate species with the increase of reaction temperature up to 150^{o}C under 3 MPa. However, a small amount of adsorbed CO species has diminished at 100^{o}C and it was never observed under the reaction condition. The experimental dynamic in situ FT-IR spectra of adsorbed species over the catalyst at various reaction conditions. This observation also suggests the direct formation of CH_3OH from CO_2 via bidentate carbonate species, formate species and methoxy species as shown in Figure 3.6

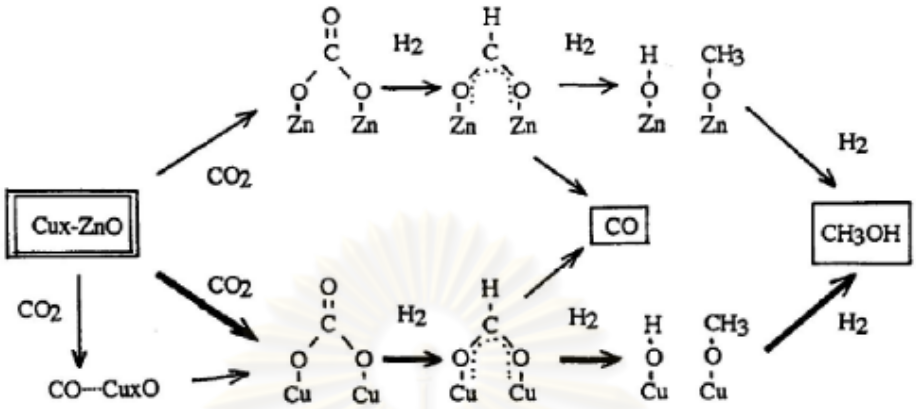

Figure 3.6: A proposed reaction mechanism for CH_3OH formation from H_2/CO_2 over Cu- ZnO/SiO_2 catalyst. [Arakawa et al., 1992]

The fibrous Cu/Zn/Al/Zr catalyst showed high activity for producing methanol from CO_2 hydrogenation [Xin et al., 2009]. Thus, there are three independent reactions present in methanol synthesis from CO_2, namely,

Methanol synthesis from CO:

$$CO + 2H_2 \rightleftharpoons CH_3OH \qquad \Delta H = -90.4 \text{ kJ/mol}$$

Reverse water gas shift:

$$CO_2 + H_2 \rightleftharpoons CO + H_2O \qquad \Delta H = +41.0 \text{ kJ/mol}$$

Methanol synthesis from CO_2:

$$CO_2 + 3H_2 \rightleftharpoons CH_3OH + H_2O \qquad \Delta H = -49.3 \text{ kJ/mol}$$

Second, Chen et al. [2009] used a commercially available Ni/Al_2O_3 sample containing K additive to enable carbon deposition from CO_2 exposure by means of catalytic hydrogenation. The experimental results suggest that K additives induce the formation of carbon nanofibers (CNFs) or carbon deposition on Ni/Al_2O_3 during the CO_2 hydrogenation reaction. These authors propose that the rate of carbon deposition depends on the reaction temperature, on H_2 and CO_2 partial pressures, and on the reactant residence time.

(1) $CO_2 + 2S \rightleftharpoons CO_2\text{-}2S$

(2) $H_2 + CO_2\text{-}2S \rightleftharpoons H_2O + CO\text{-}S + S$

(3) $H_2 + CO\text{-}S \rightleftharpoons H_2O + C\text{-}S$

Third, Lahtinen et al. [1994] investigated C, CO and CO_2 hydrogenation on cobalt foil model catalysts. It was found that the reactions produce mainly methane, but with selectivities of 98, 80, and 99 wt% at 525 K for C, CO, and CO_2, respectively. The rate of methane formation on cobalt foil shows zero order partial pressure dependence on CO_2 and first order partial pressure dependence on H_2. The reaction proceeds via dissociation of C-O bonds and formation of CoO on the surface. The reduction of CoO is the rate limiting step in the CO and CO_2 hydrogenation reaction. These authors also proposed the reaction mechanisms for C, CO and CO_2 hydrogenation. The reaction mechanisms proposed for C, CO and CO_2 hydrogenation.

C Hydrogenation	**CO Hydrogenation**	**CO_2 Hydrogenation**	
	$CO+* \Leftrightarrow CO*$	$CO2+* \Leftrightarrow CO2*$	
$H_2+2* \Leftrightarrow 2H*$	$H_2+2* \Leftrightarrow 2H*$	$H_2+2* \Leftrightarrow 2H*$	
		$CO_2*+Co \Leftrightarrow CO*+CoO$	
	$CO*+Co \Leftrightarrow C*+CoO$	$CO*+Co \Leftrightarrow C*+CoO$	$CO*+H* \Leftrightarrow COH*+*$
$C*+H* \Leftrightarrow CH*+*$	$C*+H* \Leftrightarrow CH*+*$	$C*+H* \Leftrightarrow CH*+*$	or $COH*+H* \Leftrightarrow H_2CO*+*$
$CH*+H* \Leftrightarrow CH_2*+*$		$CH*+H* \Leftrightarrow CH_2*+*$	$HCO*+Co \Leftrightarrow CH_2*+CoO$
$CH_2*+H* \Leftrightarrow CH_3*$	$CH_2*+H* \Leftrightarrow CH_3*$	$CH_2*+H* \Leftrightarrow CH_3*$	
$CH_3*+H* \Leftrightarrow CH_4+2*$	$CH_3*+H* \Leftrightarrow CH_4+2*$	$CH_3*+H* \Leftrightarrow CH_4+2*$	
	$CoO+H* \rightarrow OH*+Co$	$CoO+H* \rightarrow OH*+Co$	
	$OH*+H* \Leftrightarrow H_2O+2*$	$OH*+H* \Leftrightarrow H_2O+2*$	

CO and CO_2 methanation is investigated as an alternative purification step [Xu et al., 2006 ; Choudhury et al., 2006 ; Dagle et al., 2007]

$CO + 3H_2 \rightleftharpoons CH_4 + H_2O$ $\quad \Delta H = -206$ kJ/mol

$CO_2 + 4H_2 \rightleftharpoons CH_4 + H_2O$ $\quad \Delta H = -165$ kJ/mol

CHAPTER IV

EXPERIMENTAL

4.1 Research methodology

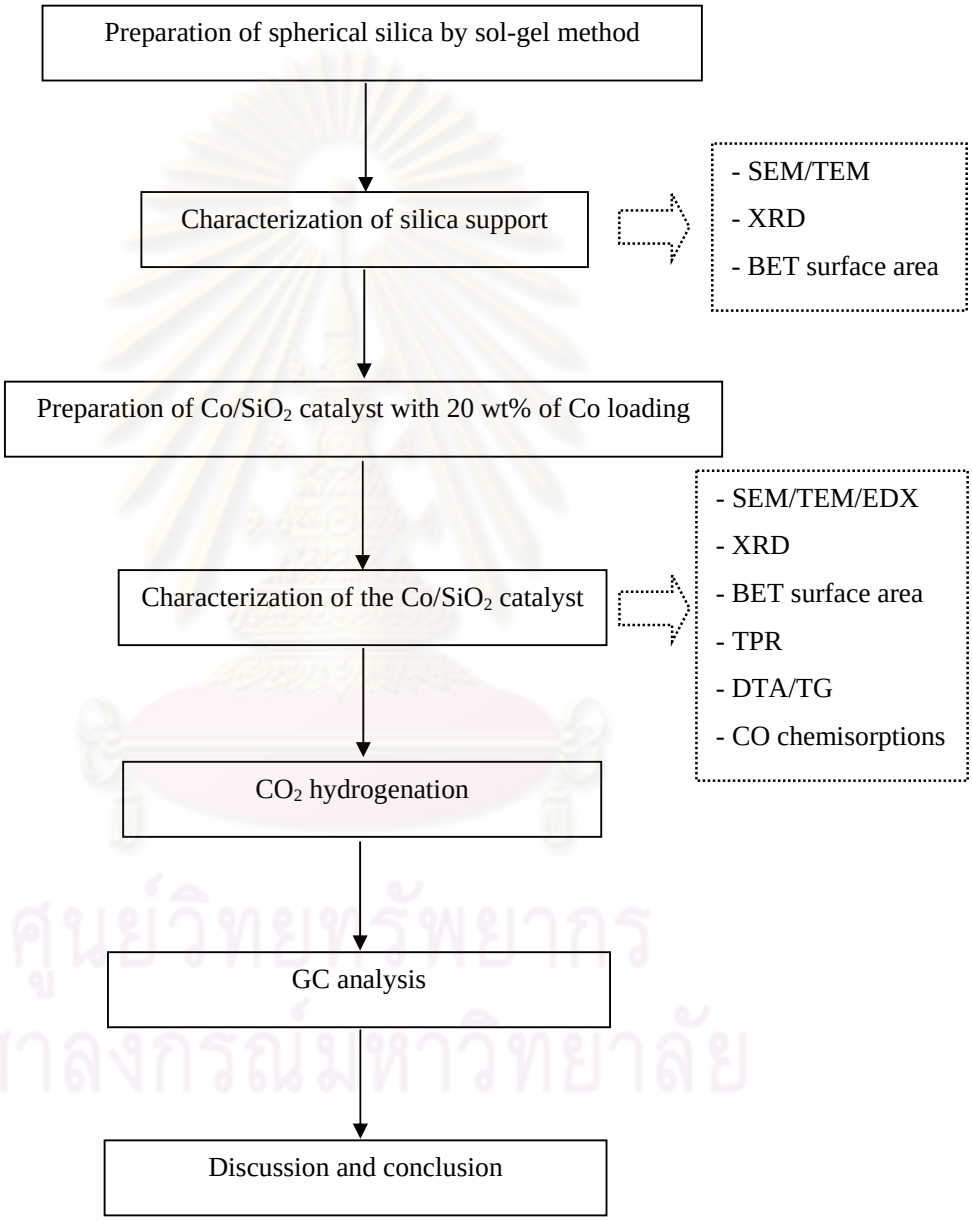

Scheme 4.1 Flow diagram of research methodology for support and catalyst 20 wt% loading

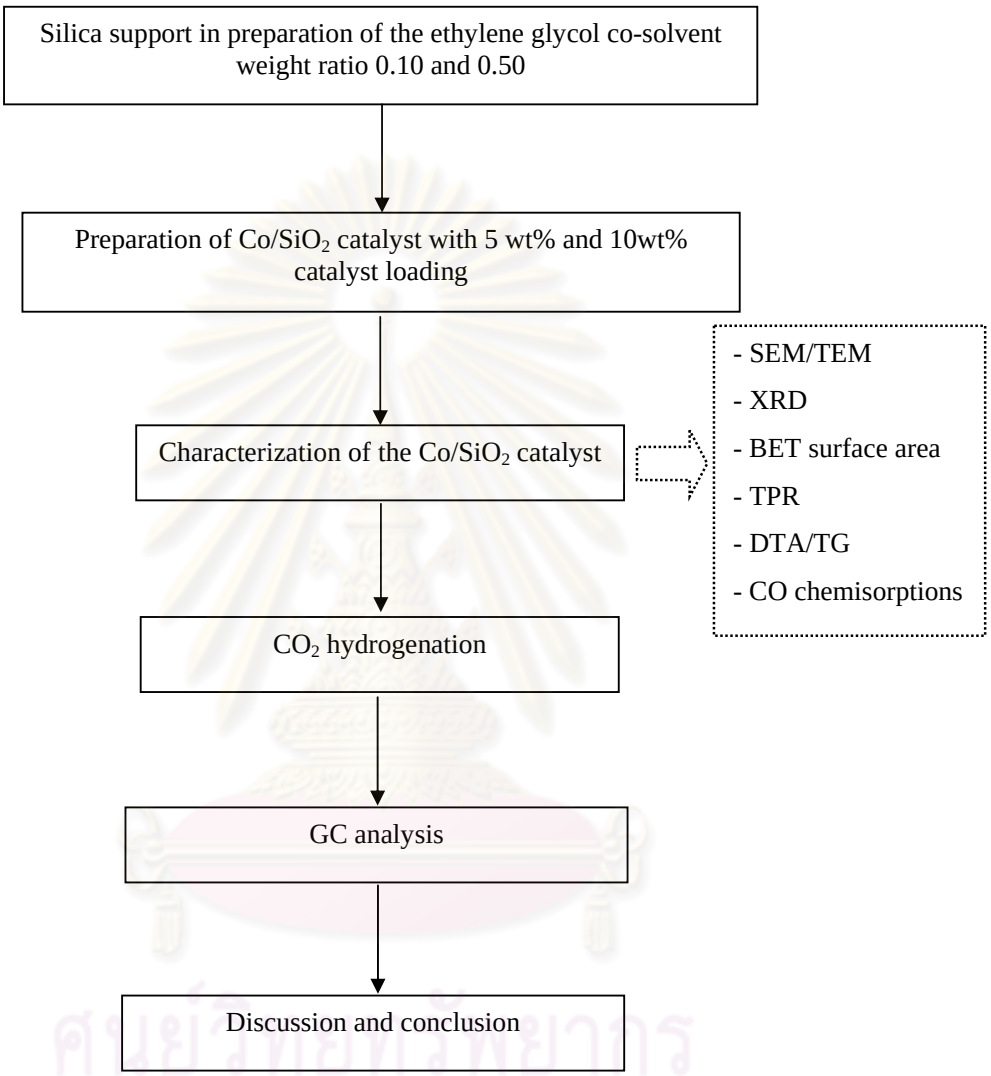

Scheme 4.2 Flow diagram of research methodology for support

and catalyst 5 and 10 wt% loading

4.2 Catalyst preparation

4.2.1 Chemical

1. Tetraethylorthosilicate 98 % (TEOS) available from Aldrich

2. Dodecyltrimethylammonium Bromide 98% (C_{12}TMACl) available from Aldrich

3. Cobalt (II) nitrate hexahydrate 98% [$Co(NO_3)_2 \cdot 6H_2O$] available from Aldrich

4. Ammonia 30% available from Merck

5. Ethanol 99.99% available from Merck

6. NaOH available from Merck

7. Ethylene glycol 99.6% available from Merck

8. Deioized water

4.2.2. Preparation of spherical silica by sol-gel method [Yamada et al., 2006]

1. The compositions of the synthesis with following 2.08 g of C_{12}TMABr and 3.74 ml of 1 M sodium hydroxide solution were dissolved in 500 g of ethylene glycol/water (25/75=w/w) solution (weight ratio 0.25). Then, 3.12 g of TEOS was added to the solution. The composition of the reaction mixture was $1SiO_2$: $0.45C_{12}$TMABr: 0.25NaOH: 133ethylene glycol: $1392H_2O$.

2. The solution was further stirred at 25°C with continuously after 8 h.

3. The white particles were filleted and wash with distillate water at least three times, and then dried the particles at 110°C for 48 h.

4. The particles obtained were calcined in air at 550°C for 6 h.

5. The silica spheres were also synthesized with different diameters by changing the weight ratio of ethylene glycol co-solvent in the range of 0.10 to 0.50 in the same sol-gel method. (7 series products)

4.2.3 Preparation of Co/SiO_2 catalysts

In this experiment, incipient wetness impregnation is used for loading cobalt. The incipient wetness impregnation procedure is as follows:

1. The certain amount of cobalt (20 wt% loading) was introduced into the de-ionized water which its volume equals to pore volume of catalyst.

2. Silica composites support was impregnated with aqueous solution of cobalt. The solution is dropped slowly to the silica composites support.

3. The catalyst was dried in the oven at 110°C for 48 h.

4. The catalyst is calcined in air at 550°C for 5 h.

5. Preparation of supported Co catalyst on the SiO_2 composites supports was synthesized by variation of the ethylene glycol co-solvent weight ratio 0.10 and 0.50 with 5wt% and 10wt% of Co by the incipient wetness impregnation as the same procedure.

4.3 Catalyst characterization

4.3.1 Scanning electron microscopy (SEM)

Scanning electron microscopy (SEM) was used to determine the morphology of the catalyst particles. Model of SEM: JEOL mode JSM-5800LV at the Scientific and Technological Research Equipment Center, Chulalongkorn University (STREC).

4.3.2 Energy dispersive X-ray spectroscopy (EDX)

Energy dispersive X-ray spectroscopy (EDX) was used to determine the morphology and elemental distribution of the catalyst particles. Model of EDX was

performed using Link Isis Series 300 program at the Scientific and Technological Research Equipment Center, Chulalongkorn University (STREC).

4.3.3 X- ray diffraction (XRD)

The bulk crystal structure and chemical phase composition were determined by diffraction of an X-ray beam as a function of the angle of the incident beam. The XRD spectrum of the catalyst is measured by using a SIEMENS D 500 X-ray diffractometer connected with a computer with Diffract ZT version 3.3 programs for fully control of the XRD analyzer. The experiments was carried out by using CuKα radiation with Ni filter in the 2θ range of 20-80 degrees resolution 0.04^{o}.

4.3.4 N_2 physisorption (BET surface area)

BET apparatus was used to measurement surface area consisted of two feed lines for helium and nitrogen. The flow rate of the gas was adjusted by means of fine-metering valve on the gas chromatograph. The sample cell made from pyrex glass. The mixture gases of helium and nitrogen was flow through the system, which was then heated up to 200^{o}C and will hold at this temperature for 1 h. After the catalyst sample was cooled down to room temperature, The mixture gases uptakes at He:N_2 ratio is a 7:3 was measured as follows.

Adsorption step: The sample that set in the sample cell was dipped into liquid nitrogen. Nitrogen gas that was flow through the system was adsorbed on the surface of the sample until equilibrium was reached.

Desorption step: The sample cell with nitrogen gas-adsorption catalyst sample was dip into the water at room temperature. The adsorbed nitrogen gas was desorbed from the surface of the sample. This step was completed when the indicator line was in the position of base line.

Calibration step: 1 ml of nitrogen gas at atmospheric pressure was injected through the calibration port of the gas chromatograph and the area was measured. The area was the calibration peak.

4.3.5 Temperature programmed reduction (TPR)

TPR was used to determine the reducibility of catalysts. Approximately 0.05 to 0.1 g of the catalyst sample was used in the operation and temperature ramping from 35^{o}C to 800^{o}C at 10^{o}C/min. The carrier gas was 5% H_2 in Ar. During reduction, a cold trap was placed to before the detector to remove water produced. A thermal conductivity detector (TCD) was measured the amount of hydrogen consumption. The calibration of hydrogen consumption was performed with bulk cobalt oxide (Co_3O_4) at the same conditions.

4.3.6 Carbon monoxide chemisorption

Static CO chemisorption at room temperature on the reduce catalysts was used to determine the number of reduce surface nickel metal atoms. The total CO chemisorption was calculated from the number of injection of a known volume. CO chemisorption was carried out following the procedure using a Micrometritics Pulse Chemisorb 2750 instrument at the Analysis Center of Department of Chemical Engineering, Faculty of Engineering, Chulalongkorn University. In an experiment, Approximately 0.10 g of the catalyst sample was filled in a glass tube. Prior to chemisorption, the catalysts was reduced at 350^{o}C for 3 hour after ramping up at a rate of 10^{o}C/min. After, carbon monoxide 30 microlite was inject to catalyst and repeat until desorption peak constant. Amount of carbon monoxide adsorption on catalyst was relative amount of active site.

4.3.7 Thermogravimetry analysis (TGA)

TGA was used to determine the weight loss pattern and the reducibility of catalysts by Shimadzu TGA model 50. The catalyst sample weights were in the range of 10-20 mg and temperature ramping from 35^{o}C to 800^{o}C at 10^{o}C/min was used in the operation. The carrier gas was H_2 UHP.

4.3.8 Transmission Electron Microscopy (TEM)

Transmission electron microscopy (TEM) was used to determine the morphology of the catalyst particles. Model of SEM: JEOL mode JSM-5800LV at the

Scientific and Technological Research Equipment Center, Chulalongkorn University (STREC).

4.4 Reaction study in CO_2 hydrogenation

4.4.1 Materials

CO_2 hydrogenation was performed using 0.1 g of catalyst packed in the middle of the stainless steel microrector, which is located in the electrical furnace. The total flow rate was 30 ml/min with the H_2/CO_2 ratio of 10/1. The catalyst sample will be re-reduced *in situ* in flowing H_2 at 350^oC for 3 h prior to CO_2 hydrogenation. CO_2 hydrogenation will be carried out at 220^oC and 1 atm total pressure. The effluent will be analyzed using gas chromatography technique [Thermal conductivity detector (TCD), molecular sieve 5 A^o was used for separation of carbon dioxide (CO_2) and methane (CH_4) and flame ionization detector (FID),VZ-10 was used for separation of light hydrocarbon such as methane (CH_4), ethane (C_2H_6), propane (C_3H_8), etc.]

4.4.2 Apparatus

Flow diagram of CO_2 hydrogenation system is shown in Figure 4.3. The system consists of a reactor, an automatic temperature controller, an electrical furnace and a gas controlling system.

4.4.2.1 Reactor

The reactor was made from a stainless steel tube (O.D. 3/8”). Two sampling points were provided above and below the catalyst bed. Catalyst was placed between two quartz wool layers.

4.4.2.2 Automation temperature controller

This unit consisted of a magnetic switch connected to a variable voltage transformer and a solid-state relay temperature controller model no. SS2425DZ connected to a thermocouple. Reactor temperature was measured at the bottom of the catalyst bed in the reactor. The temperature control set point is adjustable within the range of 0-800^oC at the maximum voltage output of 220 volt.

4.3.2.3 Electrical furnace

The furnace supplied heat to the reactor for CO hydrogenation. The reactor could be operated from temperature up to 800^{o}C at the maximum voltage of 220 volt.

4.3.2.4 Gas Controlling system

Reactant for the system was each equipped with a pressure regulator and an on-off valve and the gas flow rates were adjusted by using metering valves.

4.3.2.5 Gas Chromatography

The composition of hydrocarbons in the product stream was analyzed by a Shimadzu GC14B (VZ10) gas chromatograph equipped with a flame ionization detector. A Shimadzu GC8A (molecular sieve 5A) gas chromatography equipped with a thermal conductivity detector was used to analyze CO and H_2 in the feed and product streams. The operating conditions for each instrument are shown in the Table 4.1.

Table 4.1: Operating condition for gas chromatograph.

Gas Chromagraph	SHIMADZU GC-8A SHIMADZU	GC-14BDetector TCD FID
Detector	TCD	FID
Column	Molecular sieve 5A VZ10	VZ10
- Column material	SUS	-
- Length	2 m	-
- Outer diameter	4 mm	-
- Inner diameter	3 mm	-
- Mesh range	60/80	60/80
- Maximum temperature	350^{o}C	80^{o}C
Carrier gas	He (99.999%)	H_2 (99.999%)
Carrier gas flow	40 cc/min	–
Column gas	He (99.999%)	Air, H_2
Column gas flow	40 cc/min	–
Column temperature		
- initial (^{o}C)	60	70
- final (^{o}C)	60	70
Injector temperature (^{o}C)	100	100
Detector temperature (^{o}C)	100	150
Current (mA)	80	–
Analysed gas	Ar, CO, H_2	Hydrocarbon C1-C4

4.4.3 Procedures

1. Using 0.05 g of catalyst packed in the middle of the stainless steel microrector, which is located in the electrical furnace.

2. A flow rate of Ar = 8 CC/min, 8.8% CO_2 in H_2 = 22 CC/min and H_2 = 50 CC/min in a fixed-bed flow reactor. A relatively high H_2/CO_2 ratio was used to minimize deactivation due to carbon deposition during reaction.

3. The catalyst sample was re-reduce *in situ* in flowing H_2 at 350^{o}C for 3 h prior to CO_2 hydrogenation.

4. CO_2 hydrogenation was carried out at 220^oC and 1 atm total pressure in flowing 8.8% CO_2 in H_2.

5. The effluent was analyzed using gas chromatography technique. [Thermal conductivity detector (TDC) was used for separation of carbon dioxide (CO_2) and methane (CH_4) and flame ionization detector (FID) were used for separation of light hydrocarbon such as methane (CH_4), ethane (C_2H_6), propane (C_3H_8), etc.] In all cases, steady-state was reached within 6 h.

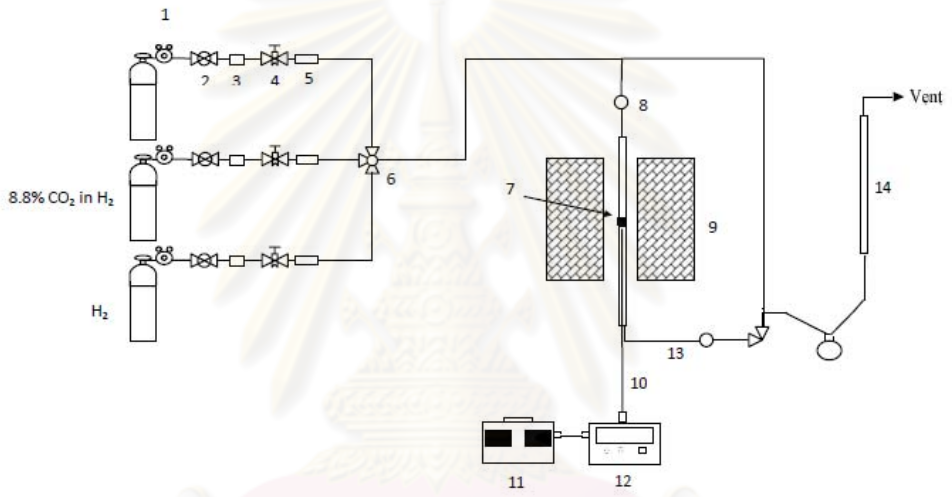

1. Pressure Regulator 2. On-Off Value 3. Gas Filter 4. Metering Valve 5. Back Pressure 6. 3-way Valve
7. Catalyst Bed 8. Sampling point 9. Furnace 10. Thermocouple 11. Variable Voltage Transformer
12. Temperature Controller 13. Heating Line 14. Bubble Flow Meter

Figure 4.3 Flow diagram of CO_2 hydrogenation system.

CHAPTER V

RESULTS AND DISCUSSIONS

This chapter was conducted in order to investigate the characteristic and catalytic properties of Co-base silica composites supported catalysts for carbon dioxide hydrogenation. This chapter is divided into three sections. The first section contains the preparation and characterization of mesoporous silica composites from sol-gel method. The second section shows characteristic and catalytic activity of silica composites supported cobalt catalyst. The last section presents characteristic and catalytic activity of silica support in preparation condition to significant result of 20%wt catalyst loading, silica support was synthesized with ethylene glycol co-solvent weight ratio 0.10 and 0.50, exhausted effect of Co loading on the silica support for Co support catalyst property.

5.1 Silica sphere with sol-gel method

Sol-gel is another technique to prepare catalysts. In the reference, the sol-gel process also allows mastering and adjusts the surface area, porosity, particle size and morphology. Thus, the sol-gel method has been known as one of easiest ways to obtain uniform structure on the particle preparation. This section describes the preparation and characterization of silica sphere particles by sol-gel method using variation of ethylene glycol co-solvent weigh ratio, respectively.

5.1.1 The morphology of silica sphere

Silica sphere was successfully synthesized with TEOS and C_{12}TMABr under diluting condition while mono-dispersed spherical particles were obtained. The morphology of silica sphere was characterized by scanning electron microscopy (SEM). The SEM images of the representative sample are shown in Figure 5.1. The sample exhibited good spherical morphology in all co-solvent ratios.

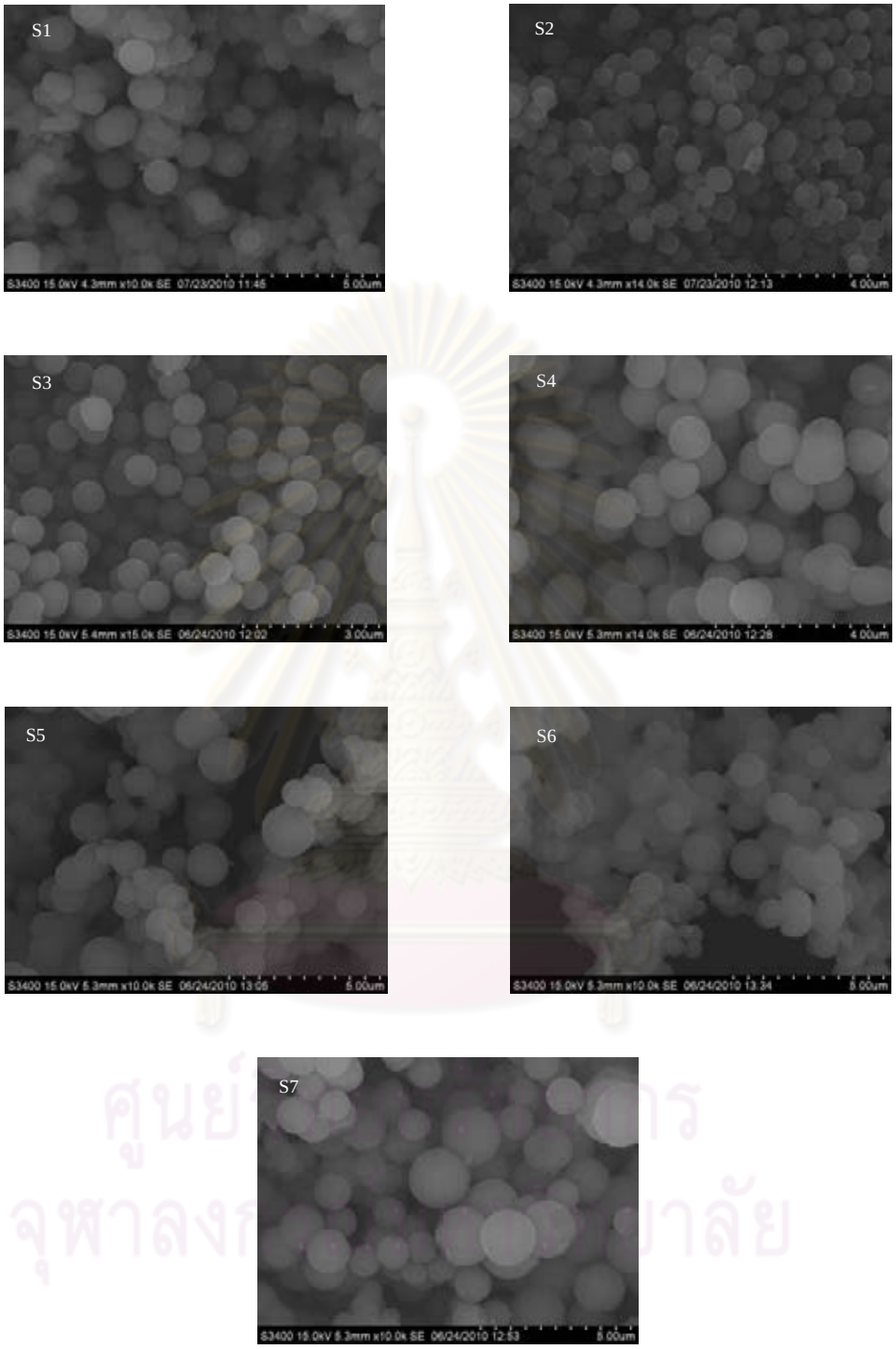

Figure 5.1: SEM images of various samples,
the name of which are denoted in Table 5.1

The internal structure of silica sphere was visualized by transmission electron microscopy (TEM). The micrograph represents the uniformly aligned radials from the center to the outside of particle. It is inferred that the mesoporous grow from the center to the outside of the sphere radially yet. In contrast, for the mono-dispersed mesoporous silica spheres synthesized with TEOS and C_{12}TMABr, the initially formed mesoporous hexagonal arrays simultaneously transformed into particles with spherical morphology [Yano and Fukushima, 2003]. Some of the TEM photographs of particles are show in Figure.5.2

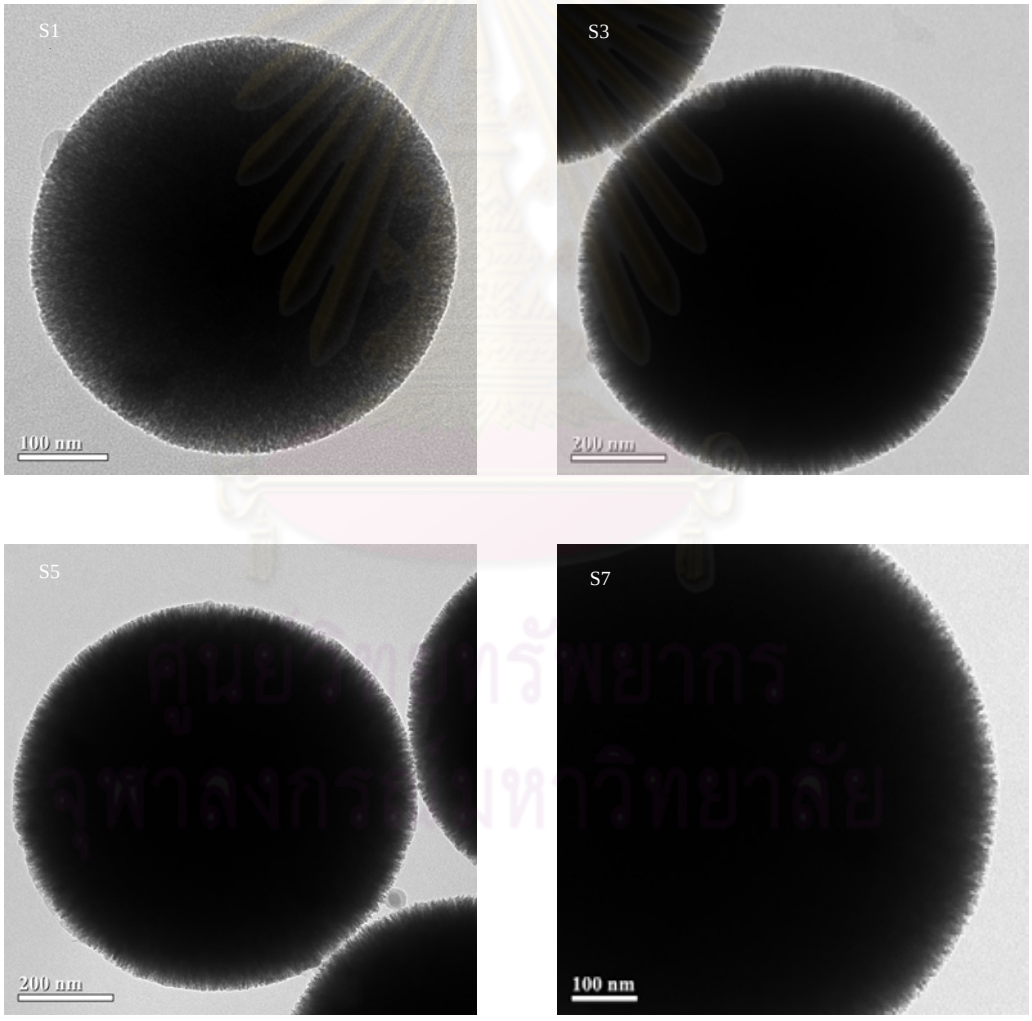

Figure 5.2: TEM images of various samples,
the name of which are denoted in Table 5.1

5.1.2 Nitrogen physisorption

The ethylene glycol weight ratio in the solvent was varied from 0.1- 0.5, which mean synthesis was conducted under rather hydrophilic and higher viscosity condition. The average diameter of the silica spheres was significantly affected by the weight ratio of ethylene glycol co-solvent used. The higher weight ratio of the co-solvent resulted in higher the size control of particle. The summarized results of the uniformity and pore characteristics of the silica spheres with the variation of co-solvent ratios are listed in table 5.1.

Table 5.1: Properties of representative spherical silica

Sample	Weight ratio of Ethylene glycol	Average particle diameter [μm]	Standard deviation [%]	Specific surface area [m^2/g]	Mean pore diameter [nm]	Pore volume [cm^3/g]
S1	0.10	0.58	21	1335	2.24	0.50
S2	0.15	0.68	9	1153	2.45	0.56
S3	0.20	0.74	5	1125	2.53	0.46
S4	0.25	1.04	5	1105	2.56	0.46
S5	0.30	1.16	28	1075	2.54	0.52
S6	0.40	1.33	30	1085	2.38	0.56
S7	0.50	1.64	35	1092	2.45	0.40

Table 5.1 was constructed in order to see that the ethylene glycol weight ratio in the solvent was variable increased from 0.1- 0.5. The average particle size decreased when the co-solvent weight ratio was reduced, but was not linearity. The size distribution uniformity was poor with the co-solvent out of range 0.15 to 0.30, an optimum co-solvent weight ratio existed for the formation of particle. All of silica spheres have high specific surface area ranging from 1000 to 1300 m^2/g. The pore size and pore volume of the silica spheres prepared using different weight ratio of co-solvent were similar in the narrow range. When the weight ratio of co-solvent was reduced until 0.1, the silica sphere leaded to increase the surface area, but the mean pore diameter was lower than other samples. However, the weight ratio of ethylene glycol hardly affected on the uniform and structure of silica sphere.

5.1.3 X-ray diffraction (XRD)

In additional, the X-ray diffraction (XRD) method could detect phase transition and phase modification of the support. From the result, the small angle X-ray diffraction (XRD) patterns of the sample exhibited one single board at (100) plane in all particles. Respectively, the boarded peak was small shifted to the higher angle and higher order peaks when the diameter of particle was changed to the larger. The slightly higher intensity indicating that the average diameters were highly order. The representative XRD patterns are depicted in Figure.5.3

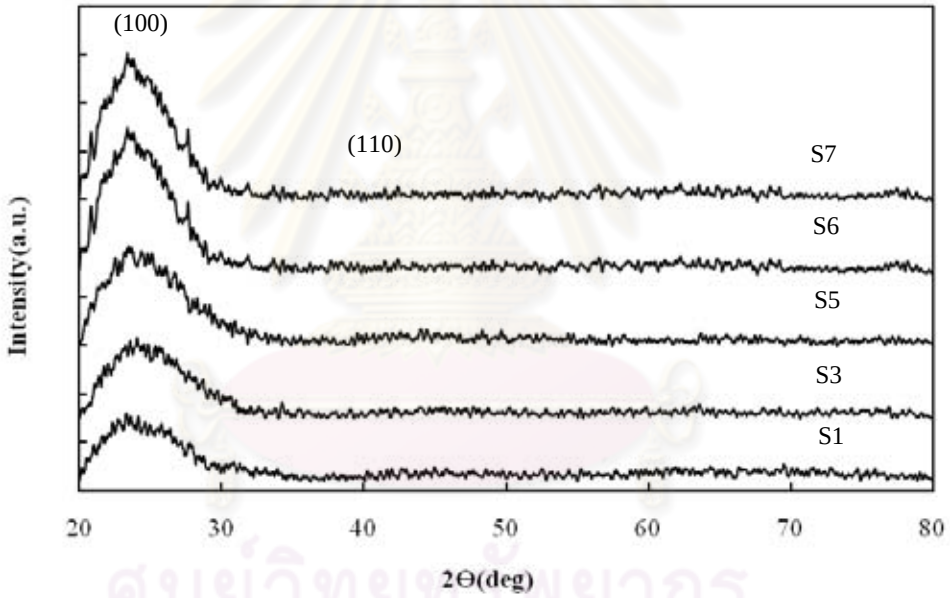

Figure.5.3: X-ray diffraction of Silica sphere with sol-gel method

5.2 Cobalt-based silica sphere (Co/SiO_2)

This section presents the characterization of cobalt-based silica sphere (Co/SiO_2). The catalyst was synthesized by variation of the ethylene glycol co-solvent weight ratio from 0.10 to 0.50 of silica support with 20wt% of Co by the incipient wetness impregnation.

5.2.1 The morphology of cobalt-based silica sphere (Co/SiO_2)

The morphology of cobalt-based silica sphere (Co/SiO_2) was characterized by scanning electron microscopy (SEM). The impregnation and calcination procedure were applied for catalyst preparation in the same of 20wt% Co loading. Therefore, the catalyst was maintained the spherical morphology and constant particle size nearly the support particle. The SEM picture was confirmed the shape and diameter of the catalyst in the Figure. 5.4

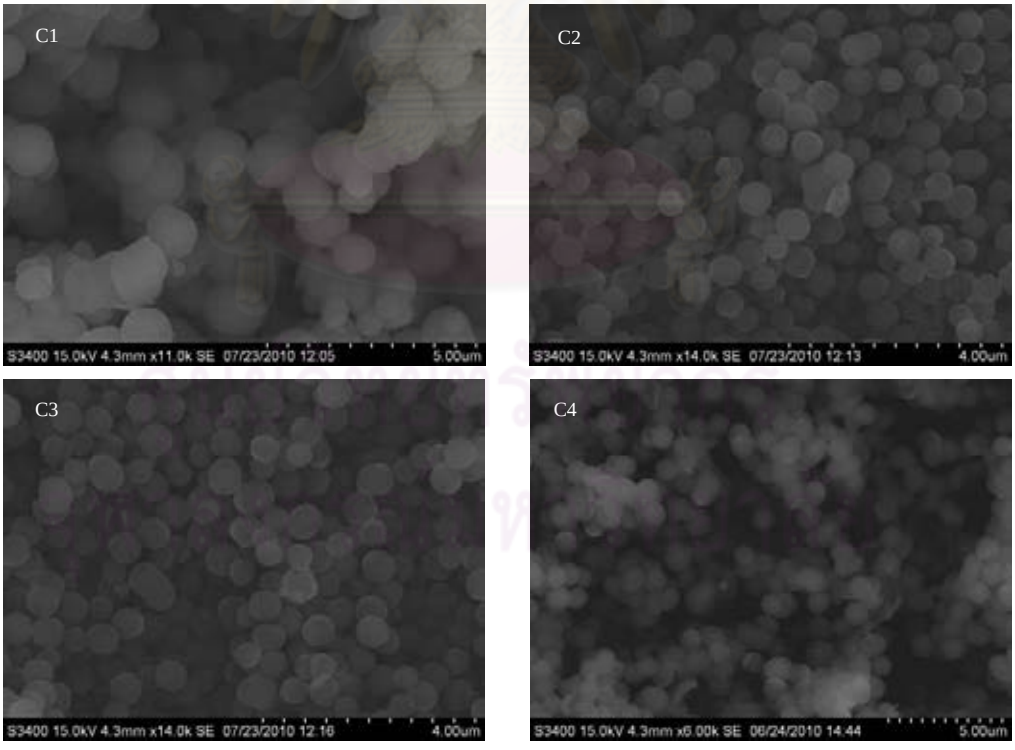

Figure 5.4.: SEM images of cobalt-based silica sphere (Co/SiO_2), the name of which are denoted in Table 5.2

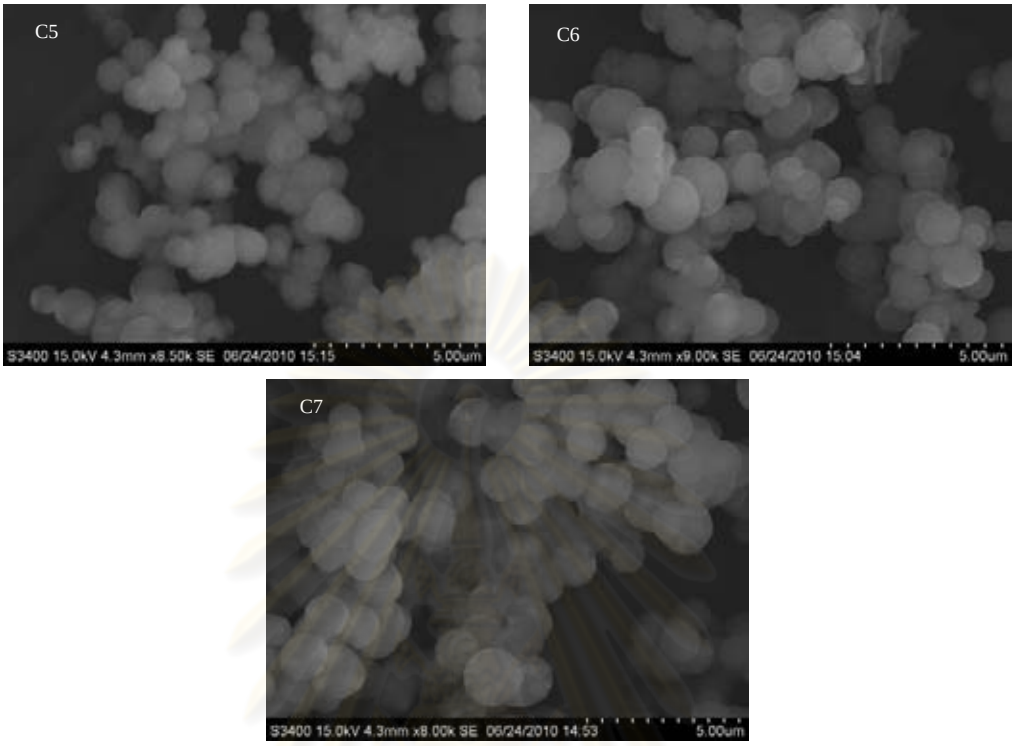

Figure 5.4(cont.): SEM images of cobalt-based silica sphere (Co/SiO_2), the name of which are denoted in Table 5.2

In order to investigate the internal morphology of cobalt-based silica sphere, TEM images were presented in Figure 5.5. TEM analysis shows that the cobalt phases distribute homogenously in the silica support. The displays referred that was also substantial coagulation of catalyst particle and the support. The disposability of catalyst on spherical silica is good and smoothness. Besides, the energy dispersive X-ray spectroscopy (EDX) was also confirmed in dispersibility of catalyst on spherical silica. Figure 5.6 shows the EDX mapping of cobalt phase good distribution on the surface. The cobalt-based silica sphere with the incipient wetness impregnation reveals regular maintained the spherical morphology.

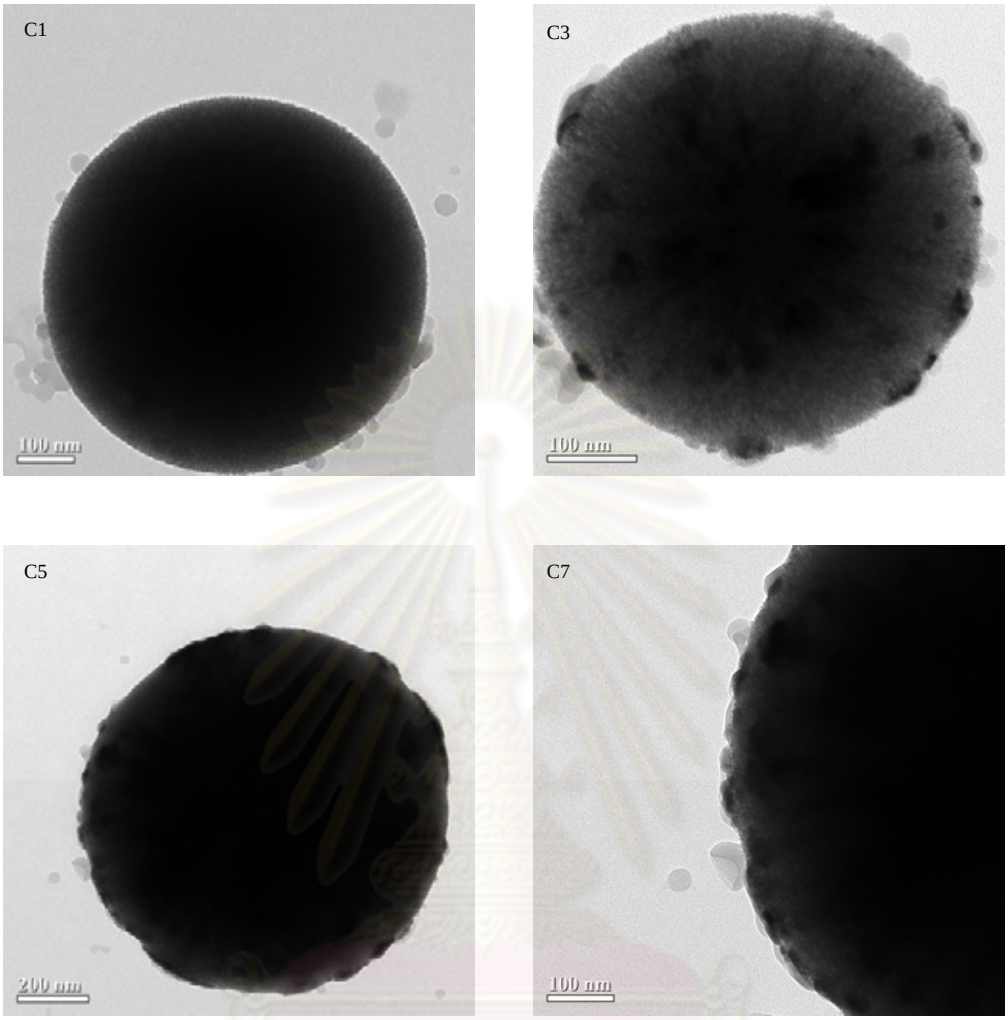

Figure 5.5: TEM images of cobalt-based silica sphere,
the name of which are denoted in Table 5.2

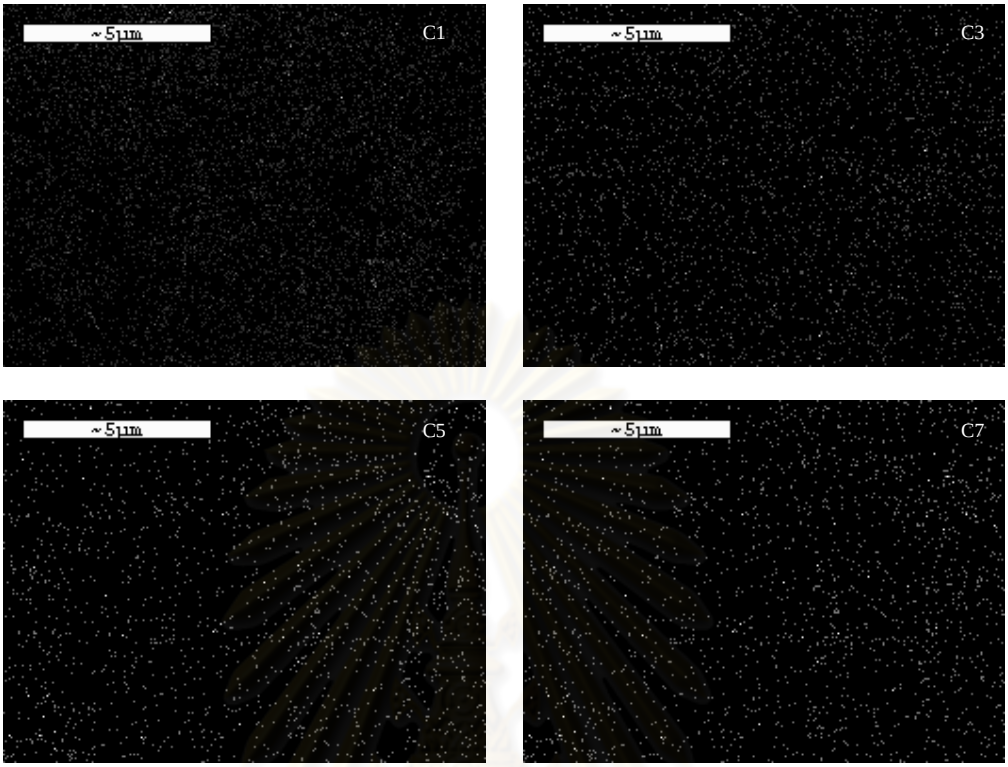

Figure 5.6: EDX mapping of cobalt-based silica sphere,
the name of which are denoted in Table 5.2

5.2.2 N_2 physisorption

The specific surface area, pore size and pore volume of spherical silica particles were measured by nitrogen physisorption technique. The adsorption isotherm is shown in table 5.2. The average particle diameter was calculated from the diameter of 50 particles observed in a SEM picture.

Table 5.2: Properties of representative Co/SiO_2 catalyst

Sample	Loading On support	Average particle diameter [μm]	Standard deviation [%]	Specific surface area [m^2/g]	Mean pore diameter [nm]	Pore volume [cm^3/g]
C1	S1	0.59	24	553	2.66	0.28
C2	S2	0.69	10	566	2.60	0.26
C3	S3	0.75	5	406	2.76	0.25
C4	S4	1.05	5	462	2.53	0.22
C5	S5	1.16	27	475	2.54	0.26
C6	S6	1.31	32	465	2.38	0.28
C7	S7	1.65	36	484	2.49	0.25

From the result, it can be observed that all samples have similar pore diameters (BJH calculation model). It is obvious that the samples possess low specific surface area and pore volume than the support. The specific surface area of catalyst was reduced about 50 percentage in range of 400 to 560 m^2/g. The highest specific surface area of catalysts was changed from catalyst C1 to C2. However, catalyst C1 and C2 had more specific surface area than other catalysts. With similar to the specific surface area, the pore volume was reduced about 50 percentage, but the mean pore diameter of catalyst was not deviated value. This is probably due to the particle substantial coagulation with crystalline catalyst. However, the catalyst was sustained the average particle diameter nearly the silica support particle. Similar to silica support, the size distribution uniformity was poor with the co-solvent out of range 0.15 to 0.30.

5.2.3 X- ray diffraction (XRD)

X- ray diffraction (XRD) is a method of characterization of solid and heterogeneous catalyst. The XRD method can be helpful for identification and characterization of the active phase. The bulk crystal structure and chemical phase composition of crystalline material having crystal domain of greater than 3-5 nm be determined by X- ray diffraction. The measurements were carried out at the diffraction angle (2θ) between 20° and 80°. The representative XRD patterns are depicted in Figure 5.7.

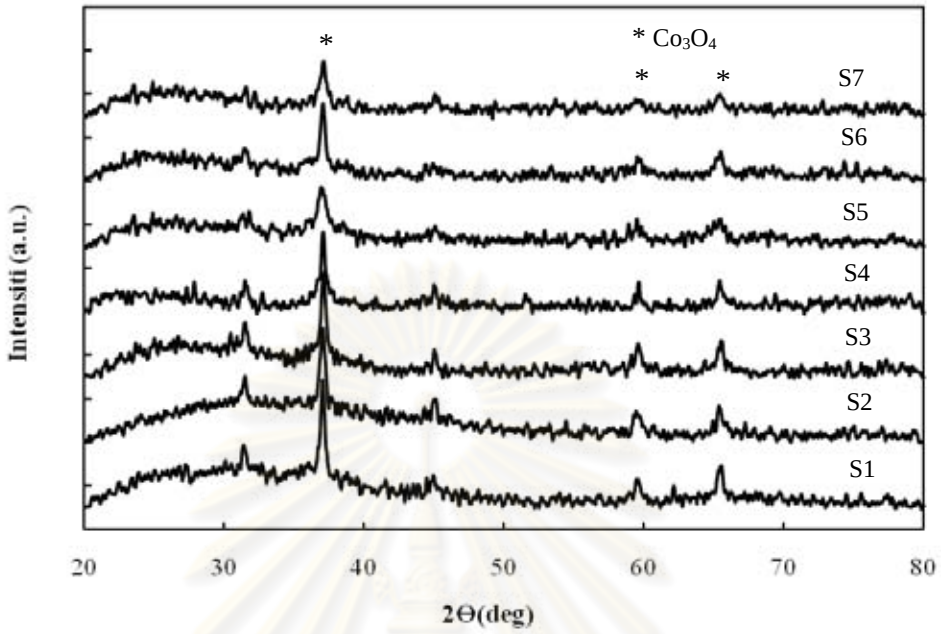

Figure 5.7: The XRD patterns of Co/SiO_2 catalyst after calcinations

The XRD patterns were collected at both lower and higher diffraction angle. Diffraction peaks at 2θ of 31°, 37°, 45°, 59.5° and 65.5° indicated that after calcinations cobalt catalyst was a crystallite. The cobalt catalyst supported by mesoporous silica sphere typically contained in the formation of crystallite Co_3O_4. The characteristic sharp peak of cobalt appeared in XRD patterns [Kodakov et al., 2006]. After loading cobalt, the refection intensity decreased greatly, but the catalyst still retained the regular mesoporous structure. [Li et al, 2006]. In the same cobalt loading, the cobalt crystallite size of catalyst C1 was the largest and decreased crystallinity due to the lower surface area. The cobalt crystalline phase was evaluated of cobalt crystallite size by using the Scherrer equation, the crystallite size obtained by XRD method are shown in table 5.3. Significant difference in crystal size obtained by BET surface area in table 5.1 result show that when the pore size diameter of catalyst decreased, the Co_3O_4 crystallite size decreased. The TEM result was appropriated that some Co_3O_4 clusters were formed outside the pore.

Table 5.3: Crystallite size of each Co/SiO_2 catalyst by Scherrer equation

Sample	crystallite size [nm]
C1	31.29
C2	27.09
C3	23.96
C4	22.62
C5	12.80
C6	24.18
C7	20.08

5.2.4 Temperature-programmed reduction (TPR)

Among the themoanalytical methods, temperature programmed reduction is most commonly used for characterizing heterogeneous catalyst. The TPR technique was performed in order to determine the reduction behaviors. The response of the TPR curve measured on silica-support sample is given in Figure 5.8.

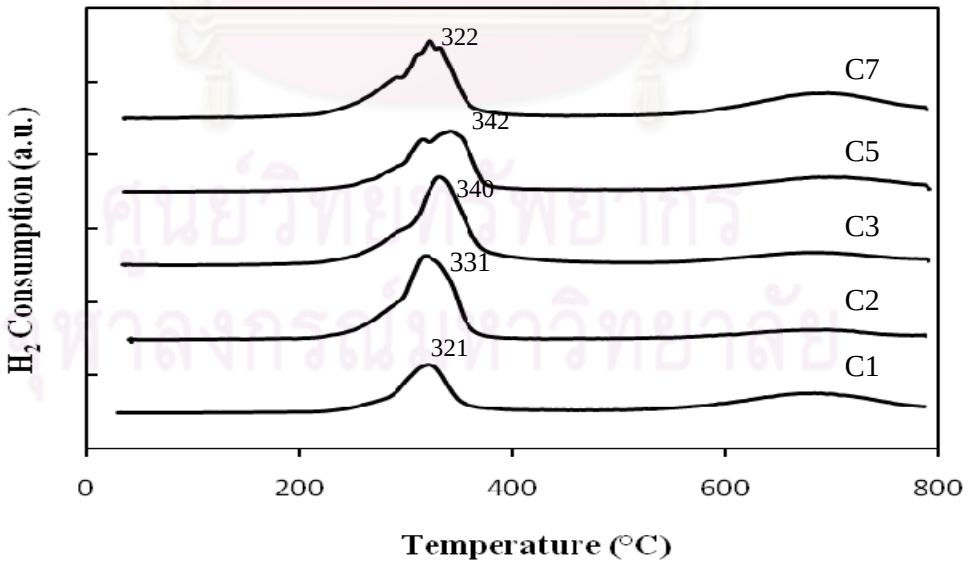

Figure 5.8: The TPR patterns of Co/SiO_2 catalyst after calcinations with 20wt% of Co

The TPR results showed that all cobalt oxide species supported on silica sphere were reduced to the metallic state by the two step of reduction. The one shoulder and one peak were detected at about 298 and 330°C, respectively, which could be assigned to the stepwise reduction of Co_3O_4.

$$Co_3O_4 + H_2 \longrightarrow 3CoO + H_2O$$
$$CoO + H_2 \longrightarrow Co^o + H_2O$$

The TPR profile of Co/SiO_2 catalyst consisted of the shoulder and one main peak, only catalyst C1 was detected in one broad peak. This broad peak could result from overlap of both reduction steps; no single steps could be ascribed to the reduction of Co_3O_4 [Kraum and Baerns, 1999]. The catalyst C5 and C7 exhibited a small peak on the top of TPR curve.

A significant increase in the reduction temperature was found for by the higher weigh ratio of ethylene glycol co-solvent with sol-gel preparation of silica support. From these profiles the maximum temperature for each catalyst is given in table 5.4. The total hydrogen consumptions of all catalysts were nearly similar in the twenty orders of magnitude. The reducibilities of the catalysts can be measured based on the peak area below TPR curve and reduction behaviors obtained from TPR results.

Usually, the interaction between cobalt and support in smaller particle is much stronger than in larger particle and this interaction is likely to stabilize small oxidized particles and clusters in silica [Khodakov et al., 2006]. In our study, the small particles had nearly diameter in the narrow microscale ranges. The interaction between cobalt and support was affected by the crystallite size of metal catalyst combined the particle size effect. From the order of crystallite size estimated by XRD signal, the sequence of decreasing small crystallite in higher weigh ratio of ethylene glycol co-solvent with support preparation was found. Interaction of smaller cobalt particles and SiOH groups in silica support may retard reduction to Co°. The larger cobalt crystallite can be easily reduced to cobalt metal [Li et al., 2006]. However, catalyst C5 seemed to against the result of H_2 consumption, which may reflect the reduction of cobalt oxide. It was probably because some cobalt crystallites existed as

very small particle inside the small pore of mesoporous silica, where H_2 consumption might have been partially blocked and undetectable.

Table 5.4: Maximum temperature and H_2 consumption from TPR profiles of each Co/SiO_2 catalyst

Sample	Reducing temperature [°C]			Total H_2 consumption	Reducibility
	Initial	Final	Maximum	[μmol H_2/g.cat]	[%]
C1	230	410	321	5.35E+20	19.66
C2	230	410	331	5.32E+20	19.59
C3	220	430	340	5.51E+20	20.23
C5	210	430	342	4.58E+20	16.83
C7	210	420	322	6.05E+20	22.21

5.2.5 Differential thermal analysis and thermogravimetric analysis (DTA/TG)

The thermal properties were characterized by thermogravimetric and differential thermal analysis (TG- DTA). TG-DTA analyses were performed under H_2 UHT carrier between 20 and 800°C for the dried catalyst. Figure 5.9 shows the DTA curve of catalyst C1 that displays several endothermic peaks below 100°C. This is due to the evaporation of physisorbed water and isopropanol solvent. The second weight loss noticeable exothermal peaks at 310°C were corresponding to the decomposition of cobalt oxide. The temperature was nearly interpreted from the TPR result. The DTA curve was similar to catalyst C1 in all cobalt-based silica sphere catalyst.

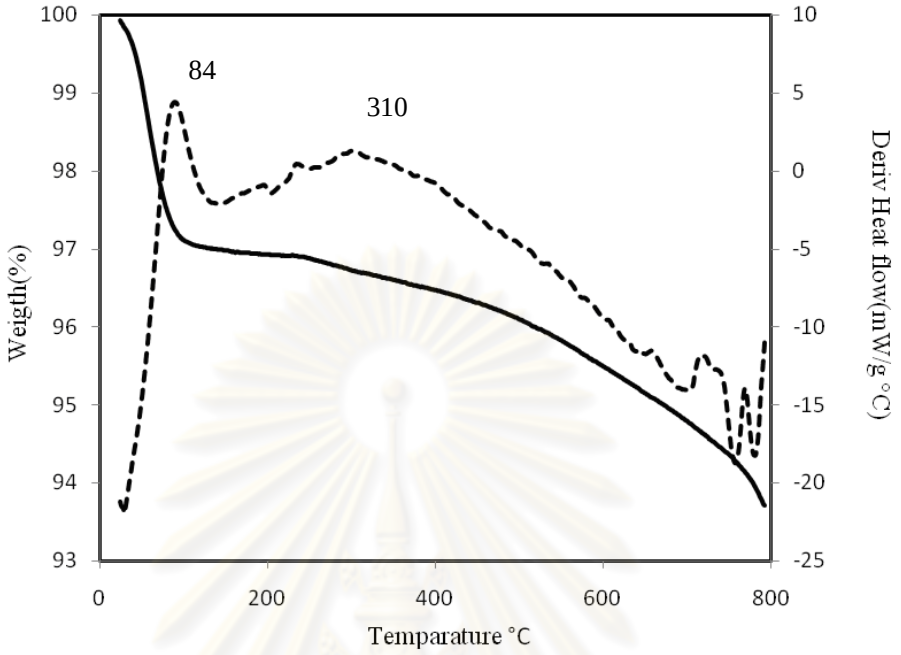

Figure 5.9: DTA/TG curve of the catalyst C1

TGA curve of each catalyst is shown in Figure 5.10. TGA curve of each catalyst displays several endothermic peaks below 100^{o}C. Similar in all catalyst, the first weight loss is attributed to the removal of physisorbed water and endothermic dehydration and second weight loss noticeable exothermal were corresponding to the decomposition of cobalt oxide. The TG curve shows a largest weight loss about 6 % in catalyst C1 and the weight loss several decease in larger particle. The weight loss can be determined by the decomposition reaction equation is 5.3 %, obtained in appendix E, nearly result about 6 % with TGA method obtained. The intrinsic reason of more specific surface area and pore volume of cobalt-based silica sphere catalyst will eventually lead to the higher evaporation of physisorbed water and isopropanol solvent.

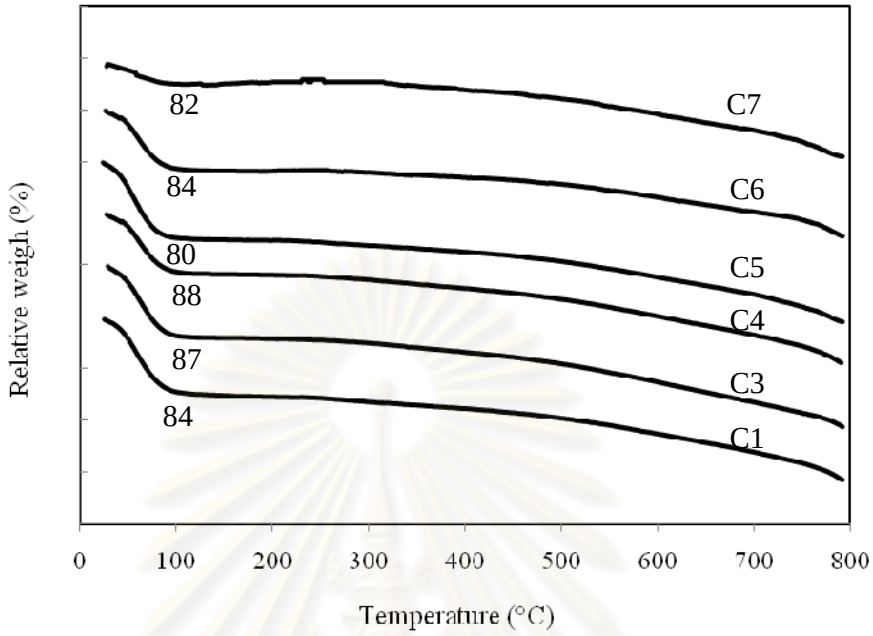

Figure 5.10: TGA curve of Co/SiO_2 catalyst

5.2.6 Carbon monoxide chemisorption

The carbon monoxide chemisorption technique was found that the carbon monoxide disproportional reaction: $2CO \longrightarrow C_{surface} + CO_2$ is a key role of simulating the first step of meachanism of the FTS, which can also be useful for comparing the catalytic activity [Moradi et al., 2003]. The catalytic active site can be calculated by amount of carbon monoxide adsorption on catalyst. Absorbed amount of carbon monoxide was directly proportional to the active site. On the other hand, the higher absorbed amount of carbon monoxide is related to the higher active site. The carbon monoxide chemisorptions results for all catalyst samples are illustrated in table 5.5. The calculation of active site of catalyst is shown in Appendix B.

Table 5.5: The CO chemisorption result of Co/SiO_2

Catalyst	Loading on support	CO Chemisorp [µmole CO/ g. Catalyst]	Active site [molecules / mole CO/m^2]	Dispersion* [%]	CO Chemisorp / BET surface area [µmole CO/g.cat/ m^2]
C1	S1	29.38	1.77E+19	0.87	0.0584
C2	S2	26.07	1.57E+19	0.77	0.0461
C3	S3	26.89	1.62E+19	0.79	0.0662
C4	S4	26.63	1.60E+19	0.74	0.0576
C5	S5	26.06	1.57E+19	0.77	0.0548
C6	S6	26.48	1.59E+19	0.78	0.0569
C7	S7	26.38	1.59E+19	0.78	0.0545

* Dispersion% base on Co loading % from impregnation technique preparation

From the result, all samples exhibited high active sites. The chemisorptions results show the similar µmole of CO that can be absorbed per gram catalyst. The catalyst C1 was represented the different performance in the chemisorptions and active site from other samples because it had large internal surface area in the term of mean pore diameter and pore volume. Besides, it had more catalyst dispersion percentage.

5.2.7 The activity test

In order to measure the catalytic behaviors of the Co supported on silica sphere supports, CO_2 hydrogenation (H_2/CO_2 = 10.36/1) under methanation condition was performed to determine the overall activity and product selectivity of the samples. Hydrogenation of CO_2 was carried out at 220°C. A flow rate of H_2 gas was purged with high purified argon at the flow rate of 8.8 ml min^{-1}. The CO_2/H_2 (8.8%CO_2) reactant was passed through the reactor at the flow rate of 21.3 ml min^{-1} to combine the argon gas in a fixed-bed flow reactor. The resulted reaction test is shown in table 5.6.

Table 5.6: Conversion and selectivity of Co/SiO_2 catalyst in CO_2 hydrogenation

Catalyst	CO_2 Conversion [a] [%]		Rate of reaction [c]	TOF [d]	CH_4 Selectivity [c]	CO Selectivity [c]
	Initial [b]	Steady state [c]	[mol CO_2/ (g cat. h)]	[x10^3 s^{-1}]	[%]	[%]
C1	9.50	9.11	4.13E-2	1.52	64	36
C2	10.40	10.42	5.58E-2	1.74	78	22
C3	22.79	17.60	9.75E-2	2.93	87	13
C4	24.51	23.53	14.27E-2	3.91	91	9
C5	26.86	20.00	12.21E-2	3.33	92	8
C6	21.63	21.50	12.73E-2	3.59	87	13
C7	20.39	21.07	12.46E-2	3.49	90	10

[a] CO_2 hydrogenation was carried out at 220°C, 1 atm, and $H_2/CO_2/Ar$ = 19.3344/1.8656/8.8, F/W= 18 L/g cat.h

[b] After 5 min of reaction.

[c] After 4 h of reaction.

[d] The TOF calculation was based on CO chemisorption.

The conversion and selectivity of cobalt-based silica sphere catalyst in CO_2 hydrogenation are shown in the table 5.5.The initial state was tested around 5 min after started reaction and the steady state was determined the average result in 3 to 6 h after started reaction. The primary major product in CO_2 hydrogenation of Co/SiO_2 catalyst is methane and only small ethane is a secondary product of reaction. The carbon monoxide intermediate was generated from the reverse water-gas shift reaction (RWGS) used to calculate the rate of reaction and selectivity. Based on results, the catalyst has nearly CO_2 conversion between initial and steady state and the conversion was larger when the particle support increased to diameter of 1.0 um. The rate of reaction and selectivity exhibited the result as same as the conversion. However, the catalyst C1 has the highest active site, but it conducted poor conversion, selectivity and rate of reaction. The CO selectivity is inverse value. The intermediate was generated from RWGS, but not to be used in the hydrogenation. The catalyst number C4 and upper exhibited good results in the activity test, perhaps due to a very small particle was pressed in to the reactor against the adsorption and increased pressure in the reactor. Therefore, there is little knowledge about CO_2 surface chemistry as

compared to CO and H_2. CO_2 is dissociate to CO and O on catalyst surface and such a process step leading to the RWGS reaction, generated CO and H_2O. CO dissociates at certain oxide-metal interface interaction. There is several researches to propose the effect of water on the activity for Co-supported catalysts in the restructuration and deactivation [Storsæter et al., 2005]. However, the main difference in the product selectivity shows the significant of the particle size distribution and uniform shape affected on the reaction.

5.3 Effect of Co loading on the silica support for Co support catalyst properties

This section describes the preparation and characterization of smallest and largest spherical silica, support S1 and S7 with different amount cobalt loading by the incipient wetness impregnation.

5.3.1 N_2 physisorption

The ethylene glycol weight ratio 0.10 and 0.50 in the co-solvent was variable with cobalt loading decreased to 10wt% and 5wt%. The summarized results of the uniformity and pore characteristics of the catalyst are listed in table 5.7.

Table 5.7: Properties of representative Co/SiO_2 catalyst verify loading

Sample	Weight ratio of Ethylene glycol	Co loading [%]	Specific surface area [m^2/g]	Mean pore diameter [nm]	Pore volume [cm^3/g]
C1	0.10	20	503	2.66	0.28
C1-2	0.10	10	663	2.34	0.29
C1-3	0.10	5	988	2.20	0.40
C7	0.50	20	484	2.49	0.25
C7-1	0.50	10	788	2.46	0.33
C7-2	0.50	5	917	2.42	0.37

Table 5.7 shows the higher specific surface area of catalyst when the amount of catalyst was increased, as same result in both silica supports. The mean pore diameter was lower with higher Co loading, but the pore size and pore volume was

inversed. The mean pore diameter was expanded to change in the big support more than small support. It showed that significant small cobalt crystalline was put in to the pore of support and may be sintering of small catalyst positive more than the bigger one. Reducing the cobalt loading sample is evident that there was also less substantial coagulation of catalyst particle on the support.

5.3.2 Temperature-programmed reduction (TPR)

The TPR technique was performed in order to determine the reduction behaviors. The response of the TPR curve measure on silica-support sample is given in Figure 5.11.

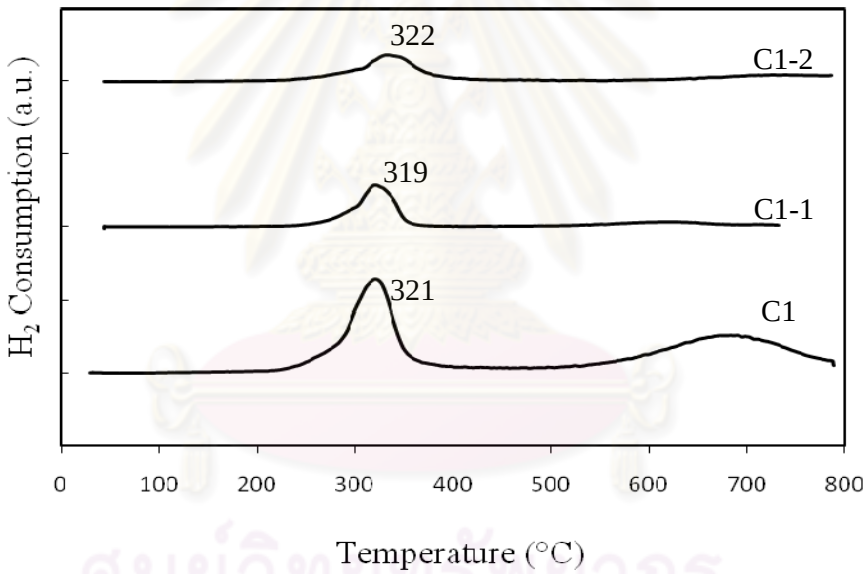

Figure 5.11: The TPR patterns of Co/SiO_2 verify catalyst loading

From the TPR result, all Co catalysts resulted in nearly of the maximum reduction temperature. The TPR profile consisted of one shoulder and one main peak, similar to those obtained for previous study with catalyst 20wt% loading. It indicated that no corresponding to the reduction between amount of cobalt loading and support. In contrast, the response of the H_2 consumption decreased and the value was very small on less catalyst loading, which can be related to the amount of catalyst loading.

However, reducibility nearly constant and higher in catalyst C1-2. The result quantitatively described by the more growth probability of Co_3O_4 distribution on catalyst surface. Table 5.8 is summarized the TPR result of catalyst C1 after decrease loading Co.

Table 5.8: TPR result Co/SiO_2 catalyst verify catalyst loading

Sample	Co loading [%]	Reducing temperature [°C] Initial	Final	Maximam	Total H_2 consumption [umol H_2/g.cat]	Reducibility [%]
C1	20	230	410	321	5.72E+20	21
C1-1	10	225	410	319	3.13E+20	23
C1-2	5	215	420	322	1.45E+20	21

5.3.3 Carbon monoxide chemisorptions

The carbon monoxide chemisorptions results for the catalyst are shown in table 5.9. From the result, catalyst has similar behavior on CO chemisorptions and active value in both different support particle sizes. However, the decreased value was very dropped when reduced the cobalt loading to 5wt% and higher affected in the small support particle size rather than the large particle. The CO chemisorp/BET surface area results were related to the CO chemisorption result with decreasing when reduced the cobalt loading.

Table 5.9: The CO chemisorption result of Co/SiO_2 verify catalyst loading

Catalyst	Loading on Support	Co loading [%]	CO Chemisorp [µmole CO/ g. Catalyst)]	Active site [molecules / mole CO/m^2]	Dispersion* [%]	CO Chemisorp / BET surface area [µmole CO/g.cat/ m^2]
C1	S1	20	29.38	1.77E+19	0.87	0.0584
C1-1	S1	10	27.78	1.67E+19	1.64	0.0419
C1-2	S1	5	8.72	5.25E+18	0.79	0.0088
C7	S7	20	26.38	1.59E+19	0.78	0.0545
C7-1	S7	10	13.66	8.22E+18	0.81	0.0173
C7-2	S7	5	10.32	6.56E+18	0.80	0.0113

* Dispersion% base on Co loading % from impregnation technique preparation

Inexpertly, the dispersion cannot explain the observed enhancement in active site. The dispersion can be maintain in the large support particle, but without significant and great uncertainty dispersion value in small support particle, indicating that there is an important of morphology of particle in the CO chemisorption when variable of amount of catalyst addition.

5.3.4 The activity test

In order to determine the catalytic behaviors of the verity of amount of cobalt supported on C1 and C7 supports, CO_2 hydrogenation (H_2/CO_2 = 10.36/1) under methanation condition was performed to determine the overall activity and product selectivity of the samples. Hydrogenation of CO_2 was carried out at 220°C. A flow rate of $H_2/CO_2/Ar$ = 19.3344/1.8656/8.8 cm^3/min in a fixed-bed flow reactor was used. The resulted reaction test is shown in table 5.10.

Table 5.10: Conversion and selectivity of Co/SiO_2 catalyst in CO_2 hydrogenation verify catalyst loading

Catalyst	CO_2 Conversion [a] [%]		Rate of reaction [c]	TOF [d]	CH_4 Selectivity [c]	CO Selectivity [c]
	Initial [b]	Steady state [c]	[mol CO_2/ (g cat. h)]	[x10^3 s^{-1}]	[%]	[%]
C1	9.50	9.11	4.13E-2	1.52	64	36
C1-1	10.23	7.16	4.06E-2	1.35	56	44
C1-2	4.12	3.41	1.15E-2	1.09	52	48
C7	20.39	21.07	12.46E-2	3.49	90	10
C7-1	16.44	10.16	5.45E-2	0.31	80	20
C7-2	4.62	4.17	1.70E-2	0.17	61	39

[a] CO_2 hydrogenation was carried out at 220°C, 1 atm, and $H_2/CO_2/Ar$ = 19.3344/1.8656/8.8, F/W= 18 L/g cat.h

[b] After 5 min of reaction.

[c] After 4 h of reaction.

[d] The TOF calculation was based on CO chemisorption.

Concomitantly, the same CO_2 conversion and rate of reaction value were decreased with lower cobalt catalyst loading. As for C7 support catalyst, the Co/SiO_2 catalyst achieves lower CO_2 conversion and rate of reaction than C1 support catalyst. In resent claimed, the results depend on the CO chemisorption and active site for reaction.

It was in accordance with the intermediate was generated from RWGS, but not to be used in the hydrogenation. The high catalyst loading shows higher CO and CH_4 selectivity. It is probably due to the byproduct water could not diffuse out of small catalyst pores quickly and the small support cobalt was not changed the chain growth of hydrocarbon product [Zhang et al., 2004].

As compare in result, support C7 showed the higher catalytic activity indicating performance in CO_2 hydrogenation than support C1 in the same catalyst loading. The activity and selectivity of the CO/SiO_2 catalyst are markedly depended on their morphology, uniformity and surface structure.

CHAPTER VI

CONCLUSIONS AND RECOMMENDATIONS

In this chapter, Section 6.1 provides the conclusions obtained from the experimental results of spherical silica synthesized by the sol-gel method. The cobalt supports on spherical silica characteristics and catalytic activity during CO_2 hydrogenation. Additionally, recommendations for further study are given in section 6.2.

6.1 Conclusions

In summary, the sol-gel method was successfully synthesized the spherical silica from TEOS and C_{12}TMABr as a surfactant template. The particle has a good shape and morphology and the particle diameter was controlled by changing the weight ratio of ethylene glycol co-solvent. The uniformity of particle diameter has a high standard deviation, when the weight ratio outside the range of 0.15 to 0.30. The 20 wt% loading of cobalt catalyst prepared by the incipient wetness impregnation on spherical silica is nearly resulting of the characterization. The specific surface area of catalyst was reduced about 50 percentage in range of 400 to 560 m^2/g. As same as the specific surface area, the pore volume was reduced about 50%, but the mean pore diameter of catalyst was not deviated value. The smaller particle of catalyst diameter has a larger surface area and active site, but poor result of the activity test of the reaction. Due to the spatial and chemical effect of support coexisting in the catalyst behavior, where uniformity and good dispersion provided higher efficiency of reactant and product exhibited in the result of ethylene glycol co-solvent weight ratio 0.25. The variation of catalyst loading significantly enhanced activity and selectivity of catalyst. The same catalyst loading was found to have a profound influence of uniformity and particle size has effect on the catalyst efficiency. Moreover, the control of the physical and morphology of support has effect on the performance of Co catalysts in CO_2 hydrogenation.

6.2 Recommendations

1. To measure of stability of catalyst after the reaction, some previous study reported that Co/Si ratio decreases after reduction and reaches practically the initial value after reoxidation [R. Riva et al., 2000], should be future obtaining the sintering probably occurring versus the particle size of cobalt support catalyst.

2. The CO_2 hydrogenation that was performed at higher temperature should be futher studied.

.

REFERENCES

Aksoylu, A.E., and Önsan, Z.I. Hydrogenation of Carbon Oxides using Coprecipitated and Impregnated Nickel-Alumina Catalysts. Appl. Catal. A 164 (1997) : 1-14.

Adesina, A.A. Hydrocarbon synthesis via Fischer-Tropsch reaction: travails and triumphs. Appl. Catal. A 138 (1996) : 345-367.

Ågren, P., and Rosenholm, J.B. Phase Behavior and Structural Changes in Tetraethylorthosilicate-Derived Gels in the Presence of Polyethylene Glycol, Studied by Rheological Techniques and Visual Observations. J. Colloid Interf. Sci. 204(1) (1998) : 45-52.

Arakawa, H. Dubois, J.L., and Sayama, K. Selective conversion of CO_2 to methanol by catalytic hydrogenation over promoted copper catalyst. Energy Convers 33 (1992) : 521-528.

Beck, J.S., and others. A new family of mesoporous molecular sieves prepared with liquid crystal templatesz. J. Am. Chem. Soc. 114(27) (1992) : 10834–10843.

Borodko, Y., and Somorjai, G.A. Catalytic hydrogenation of carbon oxides-a 10 year perspective. Appl. Catal. A-Gen 186 (1999) : 355-362.

Chang, F.W., Kuo, M.S., Tsay, M.T., and Hsieh, M.C. Hydrogenation of CO_2 over nickel catalysts on rice husk ash-alumina prepared by incipient wetness impregnation. Appl. Catal. A 247 (2003) : 309–320.

Chen, C.S., Lin, J.H., Wu, J.H., and Chiang, C.Y. Growth of carbon nano fibers synthesized from CO_2 hydrogenation on a $K/Ni/Al_2O_3$ catalyst. Catal.Commun. 11 (2009) : 220-224.

Choudhury, M.B.I., Ahmed, S., Shalabi, M.A., and Inui, T. Preferential methanation of CO in a syngas involving CO at lower temperature range. Appl. Catal. A-Gen. 314 (2006) : 47-53.

Dagle, R.A., Wang, Y., Xia, G.G., Strohm, J.J., Holladay, J., and Palo, D.R. Selective CO methanation catalysts for fuel processing applications. Appl. Catal. A-Gen. 326 (2007) : 213-218.

Davis, M.E. Ordered Porous Materials for Emerging Applications. Nature. 417 (2002) : 813.

Dry, M.E. Practical and theoretical aspects of the catalytic Fischer-Tropsch process. Appl. Catal. A 138 (1996) : 319-334.

Giakoumelou, I., Parvulescu V., and Boghosian S. Oxidation of sulfur dioxide over supported solid V_2O_5/SiO_2 and supported molten salt V_2O_5-Cs_2SO_4/SiO_2 catalysts: molecular structure and reactivity. J. Catal. 225 (2004) : 337-349.

Grün, M., Lauer, I., and Unger, K.K. The synthesis of micrometer-and submicrometer-size spheres of ordered mesoporous oxide MCM-41. Adv. Mater. 9 (1997) : 254-257.

Grün, M., Unger, K.K., Matsumoto, A., and Tsutsumi, K. Novel pathways for the preparation of mesoporous MCM-41 materials: control of porosity and morphology. Micropor. Mesopor. Mater. 27 (1999) : 207–216.

Hench, L.L., and West, J.K. The Sol-Gel Process. Chem. Rev. (1990) : 33.

Hinchiranan, S., Zhang, Y., Nagamori, S., Vitidsant, T., and Tsubaki, N. TiO_2 promotedCo/SiO_2 catalysts for Fischer–Tropsch synthesis. Fuel Processing Technology 89 (2008) : 455-459.

Iglesia, E. Design, synthesis, and use of cobalt-based Fischer-Tropsch synthesis catalysts. Appl. Catal. A 161 (1997) : 59-78.

Jongsomjit, B., Ngamposri, S., and Praserthdam, P. Catalytic Activity During Copolymerization of Ethylene and 1-Hexene via Mixed TiO_2/SiO_2 supported MAO with rac-Et[Ind]$_2ZrCl_2$ Metallocene Catalyst. J. of Molecules 10 (2005) : 603-609.

Jongsomjit, B., Wongsalee, T., and Praserthdam, P. Catalytic behaviors of mixed TiO_2-SiO_2 supported cobalt Fischer-Tropsch catalysts for carbon monoxide hydrogenation. J. Mater. Chem. 97 (2006) : 343-350.

Khodakov, A.Y., Chu, W., and Fongarland, P. Advance in the development of novel cobalt fischer tropsch catalysts for systhesis of long-chain hydrocarbons and clean fuels. Chem. Rev. 107 (2007) : 1692-1744.

Kosuge, K., and Singh, P.S. Rapid synthesis of Al-containing mesoporous silica hard spheres of 30-50 mμ m diameter. Chem. Mater. 13 (2001) : 2476-2482.

Kosuge, K., Kikukawa, N., and Takemori, M. One-Step Preparation of Porous Silica Spheres from Sodium Silicate Using Triblock Copolymer Templating. Chem. Mater. 16 (2004) : 4181-4186.

Kraum, M., and Baerns, M. Fischer-tropsch systhesis: the influence of various cobalt compounds applied in the preparation of supported cobalt on their performance. Appl. Catal. A-Gen. 186 (1999) : 189-200.

Kurganov, A., Unger, K.K., and Issaeva, T. Packings of an unidimensional regular pore structure as model packings in size exclusion and inverse size-exclusion chromatography. J. Chromatogr. A 753 (1996) : 177.

Kusama, H., Sayama, K., and Aracawa, H. CO_2 Hydrogenation to Ethanol over Promoted Rh/SiO_2 Catalysts. Catal. today 28 (1996) : 261-266.

Lahtinen, J., Anraku, T., and Somorjai, G.A. C, CO and CO_2 hydrogenation on cobalt foil model catalysts : evidence for the need of CoO reduction. Catal. Lett. 25 (1994) : 241-255.

Li, H., Li, J., Ni, H., and Song, D. Studies on cobalt catalyst supported on silica with different pore size for Fischer-Tropsch synthesis. Catal. Lett. 110 (2006) : 71-76.

Luo, Q., Li, L., Xue, Z., and Zhao, D.Y. Synthesis of nanometer-sized mesoporous oxides. Stud. Surf. Sci. Catal. 129 (2000) : 37-41.

Moradi, G.R., Basir, M.M., Taeb, A., and Kiennemann, A. Promotion of Co/SiO_2 Fischer-Tropsch Catalysts with zirconium. Catal. Commun. 4 (2003) : 27-32.

Okabe, K., Li, X., Wei, M., and Arakawa, H. Fischer-Tropsch synthesis over $Co\text{-}SiO_2$ catalysts prepared by the sol-gel method. Catal. Today 89(4) (2004) : 431-438.

Panagiotopoulou, P., Kondarides, D.I., and Verykios, X.E. Selective methanetion of CO over supported noble metal catalysts : Effects of the nature of the metallic phase on catalytic performance. Appl. Catal. A. 344 (2008) : 45–54.

Riva, R., Miessner, H., Vitali, R., and Del Piero, G. Metal-support interaction in Co/SiO_2 and Co/TiO_2. Appl. Catal. A-Gen. 196 (2000) : 111-123.

Schacht, S., Huo, Q., Voigt-Martin, I.G., Stucky, G.D., and Schüth, F. Oil-Water Interface Templating of Mesoporous Macroscale Structures. Science. 273 (1996) : 768-771.

Shunai, C., Sakamoto, Y., Terasaki, O., and Tatsumi, T. Control of Crystal Morphology of SBA-1 Mesoporous Silica. Chem. Mater. 13(7) (2001) : 2237-2239.

Somorjai, G.A. Introduction to Surface Chemistry and Catalysis. NewYork, Wiley. 1994.

Stein, A. Advances in Microporous and Mesoporous Solids—Highlights of Recent Progress. Adv. Mater 15 (2003) : 763-755.

Stöber, W., and Fink, A. Growth of Monodisperse Silica Spheres in the Micron Size Range. J. Colloid Interface Sci. 26 (1968) : 62-69.

Storsæter, S., Borg, Ø., Blekkan, E.A., and Holmen, A. Study of the effect of water on Fischer-Tropsch synthesis over support cobalt catalysts. J. Catal. 231(2005) : 405-419.

Takanabe, K., Nagaoka, K., Nariai., K., and Aika, K. Titania-supported cobalt and nickel bimetallic catalysts for carbon dioxide reforming of methane. J. Catal. 232 (2005) : 268–275.

Takenaka, S., Shimizu, T., and Otsuka, K. Complete removal of carbon monoxide in hydrogen-rich gas stream through methanation over supported metal catalysts II International. J. Hydro. Ener. 29 (2004) : 1065-1073.

Tsuneo, Y., Toshio, S., Kazuyuki, K., and Chuzo, K. The preparation of alkyltrimethyl ammonium-kanemite complexes and their conversion to microporous materials. Bull. Chem. Soc. Jpn. 63 (1990) : 988-992.

Tolbert, S.H., Schaffer, T.E., Feng, J., Hansma, P.K., and Stucky, G.D. A new phase of oriented mesoporous silicate thin films. Chem. Mater. 9 (1997) : 1962.

Yamada, Y., and Yano, K. Synthesis of monodispersed super-microporous /mesoporous silica spheres with diameters in the low submicron range. Micropor. Mesopor. Mater. 93 (2006) : 190–198.

Yang, P.D., Zhao, D.Y., Chmelka, B.F., and Stucky, G.D. Triblock copolymer directed synthesis of large-pore mesoporous silica fibers. Chem. Mater. 10 (1998) : 2033-2036.

Yang, L.M., Wang, Y.J., Sun, Y.W., Luo, G.S., and Dai, Y.Y. Synthesis of micrometer-sized hard silica spheres with uniform mesopore size and textural pores. J. Colloid Interface Sci. 29 (2006) : 823-830.

Yano, K., and Fukushima, Y. Particle size control of mono-dispersed super-microporous silica spheres. J. Mater. Chem. 13 (2003) : 2577–2581.

Xin, A., Yizan, Z., Qiang, Z., and Jinfu, W. Methanol Synthesis from CO_2 Hydrogenation with a Cu/Zn/Al/Zr Fibrous Catalyst. Chinese J. Chem. Eng. 17(1) (2009) : 88-94.

Xu, G., Chen, X., and Zhang, Z.G. Temperature-staged methanation: An alternative method to purify hydrogen-rich fuel gas for PEFC. Chem. Eng J. 121 (2006) : 97-107.

Zhang, Y., Koike, M., and Tsubaki, N. Preparation of alumina silica bimoldal pore catalysts for Fischer-Tropsch synthesis. Catal. Lett. 914 (2005) : 193-198.

Zhang, Z., Yang, L., Wang, Y., Luo, G., and Dai, Y. Morphology controlling of micrometer-sized mesoporous silica spheres assisted by polymers of polyethylene glycol and methyl cellulose. Micropor. Mesopor. Mater. 115 (2008) : 447–453.

APPENDICES

APPENDIX A

CALCULATION FOR CATALYST PREPARATION

Calculation of cobalt loading

Preparations of 20wt% Co/SiO_2 by the incipient wetness impregnation method are shown as follows:

Reagent: - Cobalt (II) nitrate hexahydrate ($Co(NO_3)_2 \cdot 6H_2O$)

Molecular weight = 291.03 g/mol

Cobalt (Co), Atomic weight = 58.933 g/mol

- Support: - spherical silica particle (SiO_2)

Based on 1.00 g of catalyst used, the composition of the catalyst will be as

Follows:

Cobalt = 0.20 g

SiO_2 = 1.00 – 0.20 = 0.80 g

Cobalt 0.20 g was prepared from Cobalt (II) nitrate hexahydrate

Cobalt (II) nitrate hexahydrate required = (0.20/58.933) x 291.03

= 0.9877 g

APPENDIX B

CALCULATION FOR TOTAL CO CHEMISORPTION AND DISPERSION

Calculation of the total CO chemisorption and metal dispersion of the catalyst, a stoischiometry of CO/Co = 1, is assumed. The calculation procedure is as follows:

Let the weight of catalyst used	=	W		g
Integral area of CO peak after adsorption	=	A		unit
Integral area of 100 µl of standard H_2 peak	=	B		unit
Amounts of CO adsorbed on catalyst	=	B-A		unit
Concentration of Co	=	C		%wt
Volume of H_2 adsorbed on catalyst	=	100 x [(B-A)/B]		µl
Volume of 1 mole of CO at 30 °C	=	24.86 x 106		µl
Mole of CO adsorbed on catalyst	= [(B-A)/B]x[100/24.86]			µmole
Total CO chemisorption	= [(B-A)/B]×[100/29.93]×[1/W]			µmole /gcatalyst
	= N			µmole /gcatalyst

$$\%\ Co\ dispersion = \frac{\text{The amount of cobalt equivalent to CO adsorption after reduction x 100}}{\text{Total amount of cobalt active sites expected to exist after reduction}}$$

Molecular weight of cobalt = 58.93

Metal dispersion (%) = 1 x CO_{tot} x 100/ [No. µmole Co_{total}]

= 1 x N x 100/ [No. µmole Co_{total}]

= 1 x N x 58.93 x 100 x 100/ [C x 10^6]

= [0.95 x N] /C

APPENDIX C

CALCULATION FOR REDUCIBILITY

For supported cobalt catalyst, it can be assumed that the major species of calcined Co catalysts is Co_3O_4. H_2 consumption to reduce Co_3O_4 is calculated as follows:

Molecular weight of Co = 58.93

Molecular weight of Co_3O_4 = 240.79

Calculation of the calibration of H_2 consumption using cobalt oxide (Co_3O_4)

Let the weight of Co_3O_4 used = 0.1 g

$= 4.153 \times 10^{4}$ mole

From equation of Co_3O_4 reduction;

$$Co_3O_4 + 4H_2 \rightarrow 3Co + 4H_2O \qquad \textit{(eq.1)}$$

Mole of hydrogen consumption = 4 Mole of Co_3O_4 consumption

$= 4 \times 4.153 \times 10^{-4}$

$= 1.661 \times 10^{-3}$ mole

Integral area of hydrogen used to reduce Co_3O_4 0.1 g = 115.63 unit

At 100 % reducibility, the amount of hydrogen consumption is 1.661×10^{-3} mole

related to the integral area of Co_3O_4 after reduction 115.63 unit.

Calculation of reducibility of supported cobalt catalyst

$$\% \text{ Reducibility} = \frac{\text{Amount of } H_2 \text{ uptake to reduce1 g of catalyst} \times 100}{\text{Amount of theoretical H uptake to reduce Co O to Co for 1 g of catalyst}} \qquad \textit{(eq.2)}$$

Integral area of the calcined catalyst = X unit

The amount of H_2 consumption = $2 \times 1.661^{-10} \times (X) / 115.63$ mole

Let the weight of calcined catalyst used = W g

Concentration of Co = Y %wt

Mole of Co = [(W x Y/100)/ 58.93] mole

Mole of Co_3O_4 = [(W x Y/100)/ (3 x 58.93)] mole

Amount of theoretical = [(W x Y/100) x 4/ (3 x 58.93)] mole

Reducibility (%) of supported Co catalyst

$$= \frac{[(2 \times 1.66 \times 10^{-3} \times (X)/115.63] \times 100}{[(0.1 \times 20/100) \times 4/(3 \times 58.93)]} \quad \text{mole}$$

Example for 20Co/ Z

Integral area of the calcined catalyst = 0.0143 unit

The amount of H_2 consumption = $[2x1.661x10^{-3}x(X)/115.63]$ *mole*

Let the weight of calcined catalyst used = 0.1 g

Concentration of Co = 20 wt%

Mole of Co = [(0.1x 20/100)/58.93] *mole*

Mole of Co_3O_4 = [(0.1x 20/100)/(3x 58.93)] *mole*

Amount of theoretical =[(0.1x20/100)x4/(3x 58.93)] *mole*

Reducibility (%) of supported Co catalyst $= \frac{[(2 \times 1.66 \times 10^{-3} \times 0.0143)/115.63] \times 100}{[(0.1 \times 20/100)X\ 4/(3 \times 58.93)]}$

= 0.8656 *mole*

APPENDIX D

CALCULATION OF THE CRYSTALLITE SIZE

Calculation of the crystallite size by Debye-Scherrer equation

The crystallite size was calculated from the half-height width of the diffraction peak of XRD pattern using the Debye-Scherrer equation.

From Scherrer equation: $$D = \frac{K\lambda}{\beta \cos \theta} \quad \textit{(eq.3)}$$

where D = Crystallite size, A

K = Crystallite-shape factor = 0.9

λ = X-ray wavelength, 1.5418 A for CuKα

θ = Observed peak angle, degree

β = X-ray diffraction broadening, radian

The X-ray diffraction broadening (β) is the pure width of a powder diffraction free from all broadening due to the experimental equipment. α-Alumina is used as a standard sample to observe the instrumental broadening since its crystallite size is larger than 2000 A. The X-ray diffraction broadening (β) can be obtained by using Warren's formula.

From Warren's formula: $$\beta = \sqrt{B_M^2 - B_S^2} \quad \textit{(eq.4)}$$

Where B_M = The measured peak width in radians at half peak height.

B_S = The corresponding width of the standard material (α-alumina).

$= (6E\text{-}7)(2\theta)^2 - (1E\text{-}5)(2\theta) + 0.0037$

Example: Calculation of the crystallite size of catalyst number C1

The half-height width diffraction peak = 0.38 ^{o} (from the figure D.1)

$= (0.38 \times \pi)/180$

= 0.0063 radian

The corresponding half-height width of peak of α-alumina

$= (6E\text{-}7)(37.00)^2 - (1E\text{-}5)(37.00) + 0.0037$

$= 0.00415$ radian

The pure width, $\beta = (0.0063^2 - 0.00415^2)^{0.5}$

$\beta = 0.0047$ radian

$2\theta = 37.00^o$

$\theta = 18.50^o$

$\lambda = 1.5418$ A

The crystallite size $= (0.9 \times 1.5418)/(0.0047 \times \text{Cos}(18.50))$

$= 312.93$ Å

$= 31.29$ nm

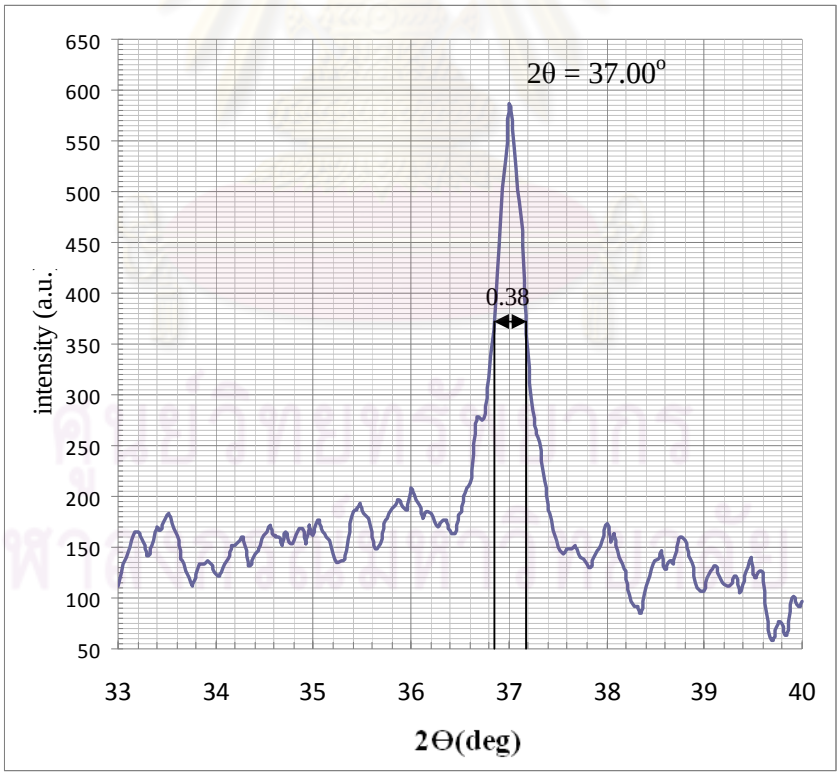

Figure D.1 The diffraction peak of catalyst number C1 for calculation of the crystallite size

APPENDIX E

CALCULATION OF THE WEIGH LOSS FROM THERMAL ANALYSIS

For supported cobalt catalyst, it can be assumed that the major species of calcined Co catalysts is Co_3O_4.

Molecular weight of Co = 58.93

Molecular weight of CoO = 75.93

Molecular weight of Co_3O_4 = 240.79

The stepwise reduction of Co_3O_4:

$$Co_3O_4 + H_2 \longrightarrow 3CoO + H_2O$$

$$CoO + H_2 \longrightarrow Co^o + H_2O$$

Calculation of the weight loss can be determined by the decomposition reaction equation:

From equation of Co_3O_4 reduction;

$$Co_3O_4 + 4H_2 \longrightarrow 3Co + 4H_2O$$

$$\% \text{ Weight loss of molecule catalyst} = \frac{(240.79 - 176.79) \times 100}{240.79}$$

$$= 26.58 \quad \%$$

Let the weight Co_3O_4 used 20 wt% of catalyst

The amount of % weigh loss of catalyst is

$$= \frac{26.58 \times 20}{100}$$

$$= 5.3 \quad \%$$

APPENDIX F

CALIBRATION CURVES

This appendix showed the calibration curves for calculation of composition of reactant and products in CO hydrogenation reaction. The reactant is CO and the main product is methane. The other products are linear hydrocarbons of heavier molecular weight that are C2-C4 such as ethane, ethylene, propane, propylene and butane. The thermal conductivity detector, gas chromatography Shimadzu model 8A was used to analyze the concentration of CO by using Molecular sieve 5A column.

The thermal conductivity detector (TCD), gas chromatography Shimadzu model 8A was used to analyze the concentration of CO2 by using porapack-Q column. The VZ10 column are used with a gas chromatography equipped with a flame ionization detector, Shimadzu model 14B, to analyze the concentration of products including of methane, ethane, ethylene, propane, propylene and butane. Conditions uses in both GC are illustrated in Table D.1.

Mole of reagent in y-axis and area reported by gas chromatography in x-axis are exhibited in the curves. The calibration curves of CO, methane, ethane, ethylene, propane, propylene and butane are illustrated in the following figures.

Table D.1 Conditions use in Shimadzu modal GC-8A and GC-14B.

Parameters	Condition	
	Shimadzu GC-8A	Shimadzu GC-14B
Width	5	5
Slope	50	50
Drift	0	0
Min. area	10	10
T.DBL	0	0
Stop time	50	60
Atten	0	0
Speed	2	2
Method	41	41
Format	1	1
SPL.WT	100	100
IS.WT	1	1

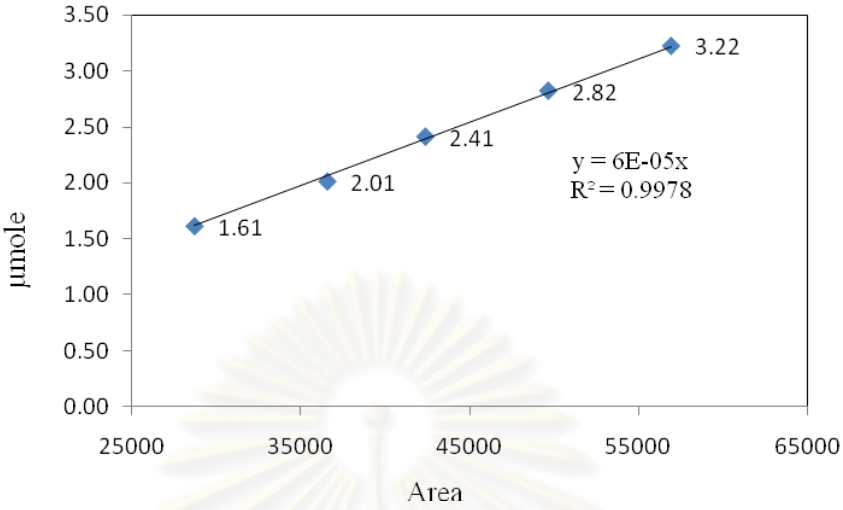

Figure D.2: Calibration curve of carbon dioxide.

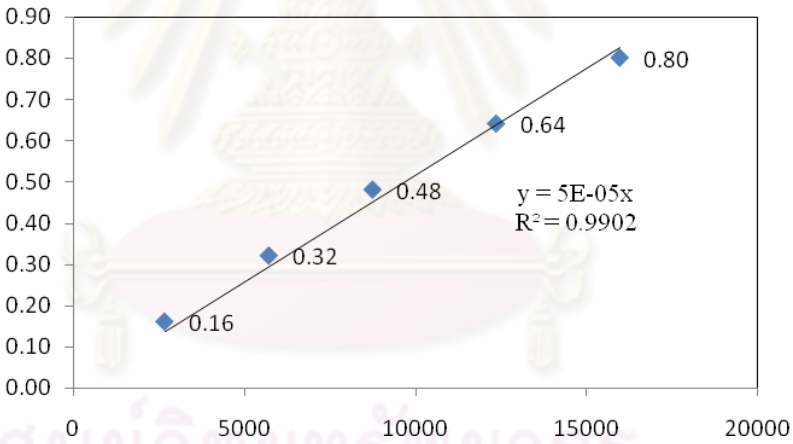

Figure D.3: Calibration curve of carbon monoxide

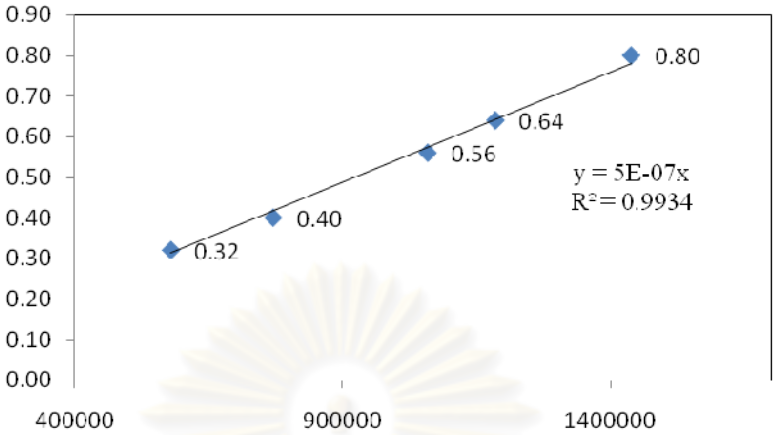

Figure D.4: Calibration curve of methane.

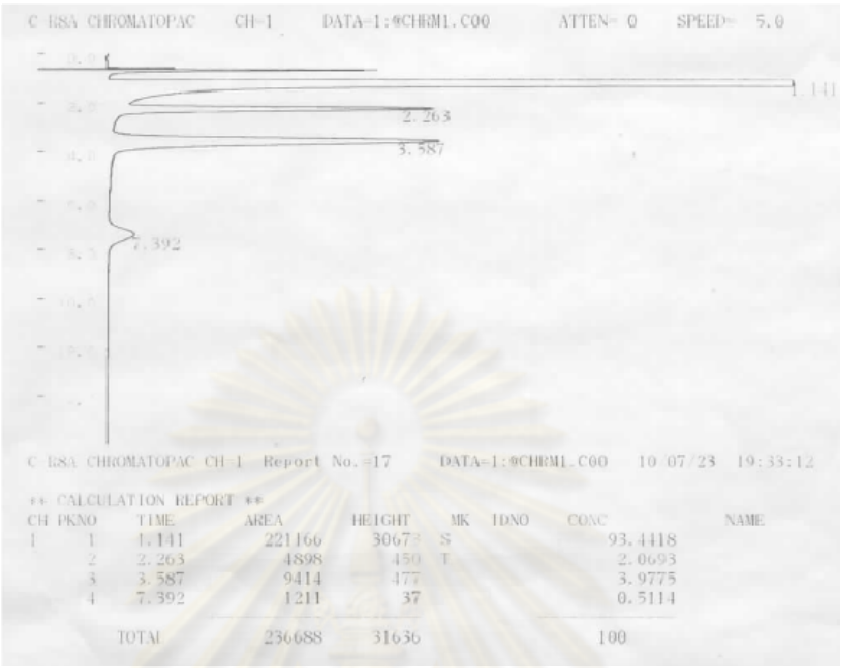

Figure D.5: Chromatograms of catalyst sample from thermal conductivity detector, gas chromatography Shimadzu model 8A (Molecular sieve 5A column).

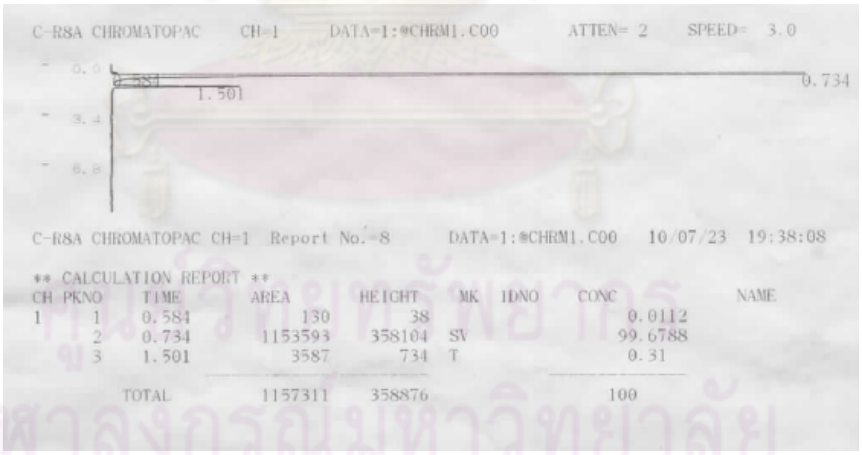

Figure D.6: Chromatograms of catalyst sample from flame ionization detector, gas chromatography Shimadzu model 14B (VZ10 column).

APPENDIX G

CALCULATION OF CO_2 CONVERSION, REACTION RATE AND SELECTIVITY

The catalyst performance for the CO_2 hydrogenation was evaluated in term of activity for CO_2 conversion, reaction rate and selectivity.

CO_2 conversion is defined as moles of CO_2 converted with respect to CO_2 in feed:

$$CO_2 \text{ conversion (\%)} = \frac{100 \times [\textit{mole of } CO_2 \textit{ in feed} - \textit{mole of } CO_2 \textit{ in product}]}{\textit{mole of } CO_2 \textit{ in feed}} \quad \text{(i)}$$

Reaction rate was calculated from CO_2 conversion that is as follows:

Let the weight of catalyst used	= W	g
Flow rate of CO_2	= 2	cc/min
Reaction time	= 60	min
Weight of CH_2	= 14	g
Volume of 1 mole of gas at 1 atm	= 22400	cc
Selectivity to CH_2	= *S*	

Reaction rate (g CH_2/g of catalyst.h)

$$= \frac{(\textit{\% conversion of } CO_2/100) \times 60 \times 14 \times 2 \times S}{W \times 22400} \quad \text{(ii)}$$

Selectivity of product is defined as mole of product (**A**) formed with respect to mole of CO_2 converted:

$$\textit{Selectivity of } \mathbf{A} \textit{ (\%)} = 100 \times [\textit{mole of } \mathbf{A} \textit{ formed /mole of total products}] \quad \text{(iii)}$$

Where A is product, mole of A can be measured employing the calibration curve of products such as methane, ethane, ethylene, propane, propylene and butane

mole of CH_4 = (area of CH_4 peak from integrator plot on GC-14B) x 8 x 1012 (iv)

VITA

Mr. Anirut Leksomboon was born on August 5th, 1979 in Suphanburi province, Thailand. He finished high school from Kannasoot Suksalai School in 1998. He received the bachelor's degree of Chemical science from Faculty of Science, Silpakorn University in 2002, respectively. He continued his master's study at Department of Chemical Engineering, Faculty of Engineering, Chulalongkorn University in June 2008.

LIST OF PUBLICATIONS

Proceeding

1. Anirut Leksomboon* and Bunjerd Jongsomjit, ''Synthesis of spherical silica by sol-gel method and its application as catalyst support.'' The 17th Regional Symposium on Chemical Engineering, Queen Silikit Nattional Convention Center, Bangkok, Thailand, November 22-23, 2010.